SynBot: An open-source image analysis software for automated quantification of synapses

Justin T. Savage[1], Juan Ramirez[1], W. Christopher Risher[2], Dolores Irala[3*], Cagla Eroglu[1,3,4,5*]

[1]Department of Neurobiology, Duke University Medical Center, Durham, NC 27710

[2]Department of Biomedical Sciences, Joan C. Edwards School of Medicine at Marshall University, Huntington, WV, USA.

[3]Department of Cell Biology, Duke University Medical Center, Durham, NC 27710

[4]Howard Hughes Medical Institute, Duke University Medical Center, Durham, NC 27710

[5]Lead contact.

*Correspondence: dolores.irala@duke.edu and cagla.eroglu@duke.edu

Keywords

image analysis, microscopy, synapse, FIJI, machine learning, immunofluorescence

Summary

The formation of precise numbers of neuronal connections, known as synapses, is crucial for brain function. Therefore, synaptogenesis mechanisms have been one of the main focuses of cellular and molecular neuroscience. Immunohistochemistry is a common tool for labeling and visualization of synapses. Thus, quantifying the numbers of synapses from light microscopy images enables screening the impacts of experimental manipulations on synapse development. Despite its utility, this approach is paired with low throughput image analysis methods that are challenging to learn, and results are variable between experimenters. We developed a new open-source ImageJ-based software, SynBot, to address these technical bottlenecks by automating several stages of the analysis. SynBot incorporates the machine learning algorithm ilastik for accurate thresholding for synaptic puncta identification, and the code can easily be modified by users. The use of this software will allow for rapid and reproducible screening of synaptic phenotypes in healthy and diseased nervous systems.

Motivation

Light microscopy imaging of pre- and post-synaptic proteins from neurons in tissue or *in vitro* allows for the effective identification of synaptic structures. Previous methods for quantitative analysis of these images were time-consuming, required extensive user training, and the source code could not be easily modified. Here, we describe SynBot, a new open-source tool that automates the synapse quantification process, decreases the requirement for user training, and allows for easy modifications to the code.

Introduction

Proper brain function relies on the correct wiring of neuronal networks[1–4]. Neuron-neuron connections, known as synapses, are the fundamental cell biological units of neural circuits[5–7]. Importantly, synapse loss or dysfunction is also a hallmark of many neurodevelopmental and neurodegenerative disorders[8–10]. Therefore, the study of synapse connectivity is crucial to understand how neuronal circuits are established during development, remodeled throughout life, and impacted by diseases.

Synapses are composed of two neuronal structures: the presynapse, located in the axon terminal, and the postsynapse, located on the dendrite. The presynapse contains specialized, neurotransmitter-filled, synaptic vesicles[6,11]. Some of these vesicles are docked at the presynaptic active zone and are fused with the membrane when an action potential reaches the synapse[11]. Neurotransmitters then diffuse into the extracellular space between the pre- and post-synapse, called the synaptic cleft[12]. Neurotransmitters in the synaptic cleft bind post-synaptic neurotransmitter receptors[13–15]. These receptors are transmembrane proteins that pass ions and/or recruit intracellular signaling partners to transduce a signal into the post-synaptic cell[7,13–15] and are anchored at the postsynapse through a scaffold of postsynaptic density proteins[16,17].

Synapses are dynamic structures that can be strengthened or lost due to changes in the inputs that neurons receive[18–20]. On the other hand, perturbations in genes that control synaptogenesis would also impact the number and organization of synaptic structures[21–23]. Non-neuronal cell types, such as astrocytes, microglia, and oligodendrocytes, also serve as critical regulators of synapse formation and elimination[24–28]. In particular, astrocytes, the major perisynaptic cells in the brain, strongly induce the

formation of excitatory and inhibitory synapses through direct contact with neuronal processes or via the secretion of several synaptogenic proteins (reviewed in [1,29–31]).

The gold standard methods for interrogating the structure and function of synapses are electron microscopy and electrophysiology, respectively. Electron microscopy (EM) allows the experimenter to visualize the synapse with a high enough resolution (~2nm) to resolve the pre- and post-synaptic compartments individually[32–34]. The characteristics of presynaptic vesicles and postsynaptic densities are used to identify excitatory versus inhibitory synapses[34–36]. An experimenter can count the number of opposing pre- and post-synaptic sites in electron micrographs of samples from various conditions to determine if these conditions alter the number of synaptic structures[34–36].

A common method for investigating synaptic function is the whole-cell patch-clamp analysis of miniature postsynaptic currents. The frequency of miniature postsynaptic currents provides information about the number of synapses a cell receives or the probability of release at the presynaptic site. On the other hand, the amplitude of these currents measures postsynaptic strength[37].

Electron microscopy and electrophysiology continue to provide high-resolution structural and functional information about synaptic physiology, but these techniques have major limitations. Firstly, both electron microscopy and electrophysiology require extensive sample preparation and specialized equipment, making them difficult to establish in a laboratory that does not specialize in these techniques. These techniques also have very low throughput and sample only a small subset of synapses or neurons, making them unsuited for screening multiple experimental conditions.

To address these limitations, higher-throughput methods for assessing synapse numbers by using immunostaining have proven useful[38,39]. These histological methods use antibodies to label pairs of pre- and post-synaptic proteins that are specialized to distinct synaptic subtypes. For example, presynaptic markers such as Vesicular Glutamate transporter 1 (VGlut1), Vesicular Glutamate transporter 2 (VGlut2), or Bassoon can be paired with postsynaptic markers Postsynaptic Density Protein 95 (PSD95) or Homer-1 to label excitatory synapses[40–44]. On the other hand, the Vesicular GABA transporter (VGAT), together with the postsynaptic Gephyrin, mark inhibitory synapses[41,45,46]. See Verstraelen et al., 2020 for a detailed comparison of synaptic marker performance[47]. When these markers are imaged using light microscopy, due to the resolution limit (200-300nm)[48], and the short (20-30nm)[44,49] distance between the pre- and post-synaptic compartments, the color signals appear to overlap at synapses.

Therefore, synaptic structures can be quantified by counting the number of colocalized pre- and post-synaptic markers using specialized image analysis software. One of the first programs for performing this analysis is the Puncta Analyzer plugin for ImageJ[38] which has been widely used in neuroscience and yielded results that were then validated through EM and EPhys[41,45,50,51]. A major limitation of Puncta Analyzer is that all steps of the analysis require user input, which can be highly subjective. Thus, image analysis using Puncta Analyzer is a lengthy process that requires extensive user training. In addition, the source code for Puncta Analyzer is quite complex and difficult to edit to allow for customization. To circumvent these technical challenges, here we developed and tested a new open-source ImageJ-based synapse analysis software we call SynBot.

Results

Synapse Labeling by Immunohistochemistry

Synapse quantification relies on the use of immunohistochemistry to fluorescently label the pre- and post-synaptic compartments (**Figure 1A**). A standard immunostaining workflow is used, including 1) fixation and permeabilization of the sample, 2) application of primary antibodies against at least one pre-synaptic and one post-synaptic marker, 3) application of fluorescent secondary antibodies against the species of the primary antibodies used, and 4) image acquisition by fluorescence microscopy (**Figure 1B**). This protocol results in images where either excitatory (**Figure 1C**) or inhibitory (**Figure 1D**) synapses can be visualized. The details of the methods are explained in the Methods section and at protocols.io (https://www.protocols.io/view/synbot-protocols-3byl4qewjvo5/v1).

Developing an automated synapse quantification tool

Our first goal in developing SynBot was to enable the efficient quantification of large imaging datasets. SynBot combines many of the image processing and analysis steps that were performed for analysis with Puncta Analyzer into one automated workflow. Toward this aim, we first developed an ImageJ macro to automate the pre-processing steps that convert raw images into numerical representations, which can be used to calculate synaptic colocalizations (**Figure 2**). First, SynBot checks the image files to determine if they are z-stacks of confocal images or single images (either single optical section from a confocal or epifluorescence image). Then SynBot processes the z-stack files to produce max projections of each 1µm stack. This step is of particular use for *in vivo* synapse number analyses, which will be discussed in detail in a later section.

Second, all images are converted to the RGB format, the color format Image J uses. Third, based on user selection, the FIJI Subtract Background, and Gaussian Blur Filter functions are applied to remove noise from the image. The fourth step is the thresholding of individual synaptic puncta to set a value for the background of the image and exclude the pixels in the image that have an intensity value less than the background. A threshold value can be determined in several different ways. The most common ones are manual thresholding and ilastik-based automated thresholding. The users can also set the threshold to a specified value. Fifth, the user decides whether to quantify synapses within a region of interest or within the whole image. After entering these user inputs, the program runs the FIJI Analyze Particles function to record the location and area of each punctum in the region of interest of the thresholded image. This function records the X and Y coordinates and area of each punctum for each color channel. Each punctum is then compared to the puncta in the other channel of the image by approximating each punctum to a circle or through a pixel-by-pixel approach discussed below.

SynBot analysis workflow

The files required for running SynBot and the installation instructions can be found at https://github.com/Eroglu-Lab/Syn_Bot. Once the Syn_Bot.ijm macro is started, a selection menu is displayed to allow the users to select their analysis parameters (**Figure 2**). The selection menu has 6 main sections: 1) Channels, 2) Preprocessing, 3) Thresholding, 4) ROI type, 5) Analysis type, and 6) Experiment Directory. The detailed functions of each option on the SynBot selection menu are defined in Table S1. Below we will summarize the utility of each section.

1) **Channels:** The fundamental objective of SynBot is to determine the overlap between different color channel objects (i.e., pre- or post-synaptic puncta). SynBot does this by first converting images into the red, green, and blue (RGB) format, which allows for consistent labeling of channels throughout the program. Users can select either the 2-channel option to analyze colocalization between the red and green channels or the 3-channel option to analyze colocalization between the red, green, and blue channels. If your images are in CMYK (cyan, magenta, yellow, and key (black)) format, or you would like to analyze red and blue or green and blue puncta colocalization, then there is also the “Pick channels” option.
2) **Preprocessing:** Images can be preprocessed after RGB conversion to reduce noise or adjust the brightness. Noise reduction is performed by applying FIJI’s subtract background plugin followed by a Gaussian blur filter to aid in object detection. Brightness adjustment changes the intensity values of each image such that there is an equal percentage of saturated pixels across images. As these methods modify the image data that SynBot will use for analysis, we advise users to apply them with caution and ensure they are producing accurate results. These modifications should also be consistent across groups of images that will be included in the same experiment.
3) **Thresholding:** One of the most challenging aspects of image analysis is thresholding, the process of distinguishing the foreground (i.e., synaptic puncta) of an image from the background. To discriminate between true synaptic puncta and the background noise is not trivial due to the small size of synaptic puncta and variability in staining and imaging parameters between users and microscopes. Therefore, here we include

a number of possible options that SynBot users can utilize. The most popular of these options is manual thresholding, where the user selects a threshold value for each channel of each image, and SynBot runs the rest of the analysis. In that sense, this option is similar to Puncta Analyzer, the predecessor of SynBot. However, we designed Synbot to have several time-saving user-friendly features. For example, Synbot automatically displays each of the image channels to be thresholded, minimizing the time required for user input. However, the manual thresholding method requires extensive user training to use properly and necessitates a significant amount of hands-on user time.

To address the limitations of manual thresholding, we implemented a new ilastik-based[52] thresholding method, where a machine learning model is used to threshold each channel of each image. ilastik is an open-source program developed by Anna Kreshuk's lab at the European Molecular Biology Laboratory. ilastik is trained by the users in a small number of images to threshold by extracting a set of user-defined features from the image and then feeding these features into a random forest machine learning model. This model is then applied to the rest of the images in the data set to determine if a given pixel is part of the foreground or background of the image. As in all thresholding methods, ilastik also requires careful troubleshooting to ensure accurate results. However, a well-trained ilastik model has a distinct advantage: it can be applied to a large number of images without the need for further user input.

We added another feature to Synbot to aid the reproducibility of results between users. All the thresholding values are saved for each image analyzed. An

analysis performed with SynBot, therefore, can be efficiently reproduced at a later date using the “Threshold From File” option. This option asks the user to supply a CSV file containing the threshold values for each channel of each image. This option does not work for ilastik because its algorithms do not use a set thresholding value.

4) **ROI Type:** SynBot’s colocalization analysis can be targeted to a region of interest (ROI) within the input image. One common application is the restriction of the analysis to the region around the soma of a cultured neuron, as in Figure 4. Alternatively, users can implement their own complex ROIs by using the FIJI clear functions to remove unwanted regions prior to running SynBot on the entire image. During the selection of the ROI, the user is also asked to input a minimum and a maximum pixel size for each channel puncta.

5) **Analysis Type:** Puncta analyzer calculated colocalization based on a circular approximation colocalization approach[38] (**Figure 3**). Therefore, we included this option also in SynBot. With the circular-approximation analysis mode selected, the coordinates and radius of each punctum for the channels to be analyzed are passed through the Syn_Bot_Helper java plugin (packaged within https://github.com/Eroglu-Lab/Syn_Bot). We used a Java plugin because it can perform the necessary calculations much more efficiently than if they were done with ImageJ macro language. These values for each punctum in the first channel are then compared to each punctum in the second channel to detect colocalizations and calculate their area using the geometry summarized in **Figure 3**. First, the distance between the centers of the two circles is calculated (**Figure 3A**). If this distance is less than the sum of the radii of the two circles, then they are counted as a colocalization, and the area of the

colocalization is calculated (**Figure 3B**). The basic idea of the area calculation is to use the two intersection points of the circles along with the center of each circle to define two triangles while also finding the areas of the sector of each circle between the two intersection points. Subtracting the area of each triangle from the area of its surrounding sector gives half of the overlapping area contributed by that punctum. This can be done for both puncta to give the total area of the overlap (co-localization)[53]. The coordinates and area of each colocalization are then stored and added to the colocalized puncta count. This method would only work if the synaptic puncta had high circularity, which can be determined using the Measure tool in FIJI and is recorded for individual puncta by SynBot. In our experience, most synaptic markers used in primary culture, or the mouse cortex are approximately circular. A table of experimental circularity values for the antibodies used in this paper is provided in Table S2.

The circular-approximation method is too slow to practically analyze three channel images and fails to correctly calculate colocalizations between non-circular objects. To overcome these limitations, here we developed a pixel-overlap colocalization method within SynBot (**Figure 3C**). Rather than approximating each punctum to a circle, this analysis mode compares puncta in a pixel-by-pixel fashion using the FIJI Image Calculator plugin's "AND" function. The AND function generates a new image that contains pixels that overlap between the red punctum and a green punctum. This new image can then be used to quantify co-localization with a third channel (blue). The coordinate and area information for colocalized puncta is then

collected. Thus, this method is more accurate and versatile and runs more quickly than the circular approximation method.

6) **Experiment Directory:** The final user input field for the SynBot selection menu is to pick a folder that contains experimental images, hereafter called the experimental directory. The directory folder should include at least one subfolder. The subfolder(s) of the experimental directory should contain only the image files to be used by SynBot. We often divide experimental groups between the subfolders of the experimental directory, but this is not required and does not affect the analysis. It is also important that image names contain only one "." character preceding their file extension. The program uses this "." to separate the file extension from the image name and will not run properly if there are multiple. Incorrect file naming can be especially problematic with some image type conversion programs that name each image with both the old and new extension (e.g., converting a Leica .lif file to .tif format can result in a name like "image1.lif.tif").

SynBot Outputs:

A key feature of SynBot is that the users can easily check if the method is counting the correct objects as colocalized puncta because after each image is analyzed, SynBot creates and saves a feedback image within the Output folder using the name of the image with "_colocs" appended to the end. This "_colocs" image shows the original input image with white circular overlays at the center position of each recorded colocalization. New SynBot users are strongly encouraged to check these images after running the macro and adjust their thresholding parameters or retrain their ilastik model if they see too few or too many calculated colocalizations that do not match what is evident by eye. The

thresholded images for each channel are also saved so the users can later validate whether each channel was accurately thresholded.

The primary output of SynBot, which contains the numbers of colocalized puncta per image, is the “Summary” csv file. This file contains the most commonly used summary measurements for synapse counting, such as the total numbers of red, green (and blue if triple colocalization is used), and the numbers of colocalized puncta from each image. The file also includes the thresholds and the settings for minimal pixel size. To allow for analysis of the cumulative properties of synaptic puncta, the macro also saves the X and Y coordinates and area of each individual puncta for the red, green, blue, and colocalized puncta into separate CSV files. These results are then ready for statistical analyses by other software such as R or GraphPad.

Quantification of Astrocyte-Induced Synaptogenesis by SynBot *in vitro.*

To test SynBot’s utility and accuracy, we used a glia-free cortical neuronal culture system[54,55]. These neurons form few synapses when cultured alone; however, astrocytes secrete proteins that strongly promote excitatory and inhibitory synapse formation in these cultures[54,55]. The synaptogenic effects of astrocyte-conditioned media (ACM) treatment are robust and promote a highly reproducible increase in the colocalization of pre and postsynaptic puncta. This histological effect has been validated by numerous studies using electron microscopy and electrophysiology[54,56–59]. Therefore, to test the utility of SynBot and compare it to Puncta Analyzer, here we used ACM treatment of purified cortical neuron cultures to induce synapse formation.

For these studies, neurons and astrocytes were individually prepared from postnatal day 1 (P1) Sprague-Dawley rat pups. First, we dissected the cerebral cortex

and performed enzymatic digestion with papain and DNAse inhibitor for 45 minutes at 32C. To stop the enzymatic digestion, we treated the tissue with ovomucoid, followed up by mechanical dissociation to obtain a single cell suspension (**Figure 4A**). This single cell suspension was then used to isolate neurons or astrocytes.

As illustrated in **Figure 4B**, neurons were purified from the single cell suspensions first through a series of negative panning steps to remove unwanted cell types in the following manner: first using Baneiraea Simplicifolia Lectin 1, we removed macrophages, second, using an anti-mouse secondary antibody-coated plate and an anti-rat secondary antibody-coated plate we removed potential non-specific Fc-binding cells such as microglia and cell debris. After the negative selection, we then incubated the cell suspension on a positive panning petri dish coated with anti-L1CAM antibody. Neonatal cortical neurons highly express L1CAM, which is absent from other cortical cell types, such as astrocytes and oligodendrocytes. Both excitatory and inhibitory neurons of the cortex are retained on the plate after incubation, and gentle washes are used to remove unbound cells. Finally, the neurons were collected from the positive-panning plate by gentle pipetting and pelleted for resuspension in neuronal growth media and plated on glass coverslips which are coated with poly-D-lysine (PDL) and laminin at a density of 70 thousand cells per coverslip.

To isolate astrocytes, we plated the cortical single-cell suspension onto a PDL-treated tissue culture flask. After 3 days *in vitro* (DIV3), we purified the astrocytes, which are tightly attached to the flask, by vigorously shaking so less-adherent cells are removed. To collect the ACM, we incubated the astrocytes with minimal media for 4 days to promote protein secretion. We collected the ACM and concentrated it using centrifugal

concentrator tubes (**Figure 4C**). After protein quantification, we applied 50ug/ml or 100ug/ml ACM to the glia-free neuronal cultures at DIV8 and DIV 11 to induce excitatory and inhibitory synapse formation, respectively (**Figure 4D**).

To label excitatory and inhibitory synapses in culture, we fixed the DIV 13 neuronal cultures and immuno-stained the synapses with pre- and postsynaptic markers. To identify excitatory synapses, we used the presynaptic active zone marker Bassoon together with the excitatory postsynaptic marker Homer1 (**Figure 4E**). To visualize inhibitory synapses, we used Bassoon in combination with the inhibitory postsynapse marker Gephyrin (**Figure 4G**). For image acquisition, we took single focal plane images using an inverted Olympus FV3000 confocal laser scanning microscope with a 60X oil immersion objective. The images were taken in a 1024X1024 resolution with a 2X digital zoom. To identify individual neurons, we used the DAPI channel, and we imaged only the neuronal cell bodies at least two cell diameters distant from other neurons. We used this strategy to avoid overlapping cells and to use an unbiased method to select the neurons to image. We imaged at least 20 cells for each condition, and the laser power for each channel was adjusted such that the signal for each channel was bright without many saturated pixels.

To determine the efficiency of SynBot to detect pre- and postsynaptic colocalization, we analyzed images from cortical neurons treated with ACM or cultured in growth media only (named here as control) using manual and ilastik thresholding methods of SynBot. We compared these results to analyses done by its predecessor Puncta, Analyzer (**Figure 4E-H**). To aid with these comparisons, we normalized the number of excitatory synapses between the ACM-treated neurons to the control values. As

expected, ACM induced a significant increase in synapse numbers (~1.5-fold) with each of the analysis methods used (student's t test $p = 0.005$, $p = 0.004$, and $p = 0.010$ for Puncta Analyzer, SynBot Manual, and SynBot ilastik, respectively) (**Figure 4F**). Similarly, we found a 2-fold increase in the numbers of inhibitory synapses when neurons were treated with ACM compared to the control (student's t test $p < 0.001$ for each analysis method) (**Figure 4H**). These results indicate that SynBot is equally efficient in detecting both types of synaptic contacts as the Puncta Analyzer. Moreover, these results show that ilastik method of thresholding can be used to determine changes in synapse numbers.

To determine whether manual or ilastik-based thresholding affected the numbers of puncta identified, we also compared the raw numbers of green (presynaptic marker), red (postsynaptic marker), and colocalizations identified between the Puncta Analyzer, SynBot Manual, and SynBot ilastik. When compared to the Puncta Analyzer and SynBot Manual, SynBot ilastik method consistently identified larger numbers of green, red, and colocalized puncta from all the images, regardless of the antibodies used or the treatment conditions (**Figure S1**). This result is consistent with ilastik's ability to detect individual objects (here punctum) based on multiple features. In contrast, manual thresholding only uses intensity cutoffs and minimal puncta size as features for detection. Together these results show that SynBot, with its user-friendly and timesaving features, efficiently detects excitatory and inhibitory synaptic contacts *in vitro*.

Quantification of *In Vivo* Excitatory Synapse Numbers by SynBot

After validating the use of SynBot *in vitro*, we next tested its utility in quantifying synapse numbers from mouse brain tissue sections. Immunohistochemistry of brain

tissue sections is a common method for synapse number quantification[40,41,45,46,55,60]. However, these analyses have the considerable added complexity of a 3-dimensional tissue section that should be imaged. Moreover, thick tissue sections from the brain inherently have more background signals, which can impair the accuracy of the analyses. Finally, antibody penetration into the tissue sections is an important consideration while optimizing synapse staining and imaging procedures. Before using SynBot or any other method, the experimenters should optimize their staining and imaging procedures. The optimized synapse staining and imaging procedure we have used can be found in the Methods section and at protocols.io (https://www.protocols.io/view/synbot-protocols-3byl4qewjvo5/v1).

To test SynBot's efficacy and accuracy in quantifying synapse numbers in vivo, we next analyzed images that were previously acquired and reported in a study by Risher and colleagues in 2018[60]. This paper showed that the neuronal Thrombospondin/Gabapentin receptor α2δ-1 is crucial for proper excitatory synapse formation in the developing mouse cortex[57,60,61]. Risher et al., 2018 showed that when in α2δ-1 KO animals, there is a significant and substantial decrease in Vglut1/PSD95 synapse numbers compared to WT controls[60]. Risher et al. validated these histological findings of impaired synaptogenesis using electrophysiology and electron microscopy that also showed a strong decrease in excitatory synapse function and number, respectively.

To perform these experiments, mice were transcardially perfused with 4% paraformaldehyde, and brains were collected, frozen, and cryosectioned (**Figure 5A**). Intracortical excitatory synapses were marked with the pre- and post-synaptic markers

specific for these connections, namely vesicular glutamate transporter 1 (VGluT1) and postsynaptic density 95 (PSD95) (**Figure 5B**). Images were acquired using a Leica SP5 confocal microscope. A z-stack of 15 optical planes was acquired using a 0.34 um z-step to image ~ 5 um of the sample. Images were acquired such that confocal settings were optimized on control conditions with the goal of minimizing oversaturated pixels but maintaining real synaptic puncta. For detailed procedures see the Methods section and protocols.io (https://www.protocols.io/view/synbot-protocols-3byl4qewjvo5/v1).

We took advantage of this well-validated data set to test SynBot's efficacy for quantifying synapse numbers in mouse brain tissue images. We reanalyzed the P21 α2δ-1 WT and KO images previously published in Risher et al., 2018 using the SynBot manual and SynBot ilastik thresholding methods and compared these to the results Risher et. al. obtained using Puncta Analyzer (**Figure 5C**). All 3 methods found a significant ~50% decrease in the number of synapses in α2δ-1 KO animals when compared to WT littermates (linear mixed effects model, $p < 0.001$ for each method). In our hands, a pre-trained Ilastik model implemented in SynBot was able to perform as well as a trained manual user (**Figures 5C and S1)**. Overall, quantification using SynBot manual thresholding and Ilastik thresholding recapitulated the previously validated finding that α2δ-1 KO mice have fewer intracortical synapses than WT littermates. This demonstrates that SynBot can be successfully applied to brain tissue images and that the thresholding methods packaged in SynBot can be used to quickly compare different strategies.

Discussion

Quantification of synapse numbers using immunohistochemistry is a favored technique for its ability to label synapses quickly and easily. However, this rapid experimental protocol was paired with slow analysis methods that were difficult to learn and often resulted in variability between users. SynBot overcomes many of the shortcomings of its predecessor by being easy to learn with built-in and online instructions and easy to use with a user interface that simplifies and streamlines user input. SynBot also allows for unsupervised analyses through its automated analysis methods, allowing the easy replication of automated or manual analyses between users. SynBot also collects all the data extracted from synaptic images by recording the position and area of each individual punctum from each image channel. These data can be used for other forms of analyses, such as the count and sizes of individual synaptic puncta or the spatial relationship in their distribution across the tissue imaged.

One of the most challenging aspects of analyzing these data is the inconsistency and subjectivity introduced by the simple manual thresholding used in the Puncta Analyzer. The six thresholding modes available in the SynBot address this by providing the user with simple approaches like a fixed threshold value or streamlined manual thresholding as well as complex machine learning-based algorithms like ilastik or others applied outside of SynBot. We have found ilastik to be particularly suited to this workflow as a short training session in ilastik is sufficient to analyze images accurately and reproducibly without the need for further user input. The details about how to train ilastik for synaptic puncta detection can be found at the Methods section and protocols.io (https://www.protocols.io/view/synbot-protocols-3byl4qewjvo5/v1). When used in the

manual mode, SynBot also automatically saves the threshold values applied to each image with the output data, allowing for rapid replication of the analysis by other users.

The advantage of implementing SynBot in the ImageJ macro language is the ease with which it can be changed by users to apply to a wider variety of experimental questions. All the source code for the macro is available on our lab GitHub site (https://github.com/Eroglu-Lab/Syn_Bot) and can be edited within FIJI itself without the need for software development programs or in-depth computer science experience. There were only a few parts of SynBot that could not be implemented in ImageJ macro language (circular-approximation colocalization, some dialog menus, ilastik integration) and required Java programming. These sections are stored in a separate ilastik4ij_Syn_Bot (https://github.com/Eroglu-Lab/ilastik4ij_Syn_Bot) repository on our lab GitHub site, which is freely available for download and can be edited by users with experience in Java programming.

With all of these features, researchers will be able to rapidly screen experimental conditions that alter synapse numbers and can move on to in depth structural and mechanistic investigations with other methods such as electrophysiology, super-resolution microscopy, or electron microscopy. Therefore, SynBot may aid in answering many outstanding questions related to synapse development and maintenance.

Limitations of the Study

There are a few key conditions necessary for SynBot to be applied. First, the signals being analyzed need to be punctate rather than diffuse since SynBot performs object-based colocalizations and must be able to identify discrete objects. Second, objects within the images must be non-overlapping to be independently counted. Third,

SynBot also only works on single optical sections or Z-stack projections and is unable to fully incorporate 3-dimensional synapse structures as is done in other software such as Imaris. With those caveats in mind, SynBot is widely applicable to any object-based colocalization analysis for synapses or any other set of imaging markers.

It is also important to note that the accuracy of synapse number analyses is heavily dependent on the quality of staining and imaging. Moreover, proper markers should be used to label synapses. Some common mistakes are to use an axonal or dendritic marker, such as GAD65 or GAD67 (for inhibitory axons) or MAP2 (for neuronal dendrites), as one of the synaptic compartments. These kinds of markers are often extrasynaptically localized and widely distributed, thus would yield co-localization with other markers even if they were not at an actual synapse.

Acknowledgments:

We thank Christabel Tan, M. Pia Rodriguez-Salazar, Dr. Oluwadamilola Lawal, Nicholas Brose, Gabrielle Sejourne, Kavya Raghunathan and other Eroglu lab members for critical feedback about the manuscript. This work was supported NIH R01 funding AG059409, NS102237, and BRAIN Initiative funding U19NS123719 and a Chan Zuckerberg Initiative, Neurodegeneration Challenge Network Collaborative grant (2018-191999 and DAF2021-237435) and by the joint efforts of MJFF and the Aligning Science Across Parkinson's (ASAP) initiative. MJFF administers the grant [ASAP-020607 to CE] on behalf of ASAP and itself Michael J Fox Foundation. D.I. was supported by The Pew Latin American Fellows Program in the Biomedical Sciences, Foerster-Bernstein Post-Doctoral Fellowship Program for Women in STEM, and the Holland-Trice Scholars Award for high

risk/high impact discovery in research in Basic Brain Science and Brain Diseases. JJR was supported by NIH funding NS102237-S1 and F31NS125985. Dr. Cagla Eroglu is an HHMI Investigator. The cartoon of a synapse in Figure 1 and a diagram of mouse brain tissue staining in Figure 5 were created using BioRender.com.

IP rights notice

This article is subject to HHMI's Open Access to Publications policy. HHMI lab heads have previously granted a nonexclusive CC BY 4.0 license to the public and a sublicensable license to HHMI in their research articles. Pursuant to those licenses, the author-accepted manuscript of this article can be made freely available under a CC BY 4.0 license immediately upon publication.

Author Contributions

Conceptualization, J.T.S. and C.E.; Software, J.T.S.; Investigation, J.R., W.C.R., and D.I.; Writing – Original Draft, J.T.S., J.R., D.I., and C.E.; Writing – Review & Editing, J.T.S., J.R., D.I., and C.E.

Declaration of Interests

The authors declare no competing interests.

Figure Legends:

Figure 1: Labeling of synapses as apposing colocalization of pre- and post-synaptic markers:

A) Illustration of excitatory and inhibitory synaptic structures. Presynaptic markers used in this paper are shown in green and postsynaptic markers are shown in magenta.

B) Synaptic staining workflow.

1. After fixation with 37°C PFA 4%, the neurons are permeabilized and non-specific epitopes are blocked in antibody buffer containing 50% NGS and 0.2% Triton X-100.
2. Neurons are incubated with primary antibodies targeting pre- and post-synaptic compartments of excitatory or inhibitory synapses.
3. After overnight incubation with primary antibodies, the neurons are washed with PBS.
4. Neurons are incubated with secondary antibodies conjugated to Alexa fluorophores.
5. After 2 hours of room temperature incubation with secondary antibodies, neurons are again washed with PBS and the neuronal nuclei are stained with DAPI.
6. Coverslips are mounted on glass slides using a medium that protects from bleaching of Alexa fluorophores for imaging.

   For details, check the Methods section and protocols.io.

C) Representative image of excitatory synapses made onto a cultured cortical neuron stained with Homer1, Bassoon, and Vglut1. The scale bar in the larger image represents 20 µm, and the scale bar in the smaller image represents 5 µm.

D) Representative image of inhibitory synapses made onto a cultured cortical neuron stained with Gephyrin, Bassoon, and VGAT. The scale bar in the larger image represents 20 μm, and the scale bar in the smaller image represents 5 μm.

Figure 2: Workflow for SynBot synapse quantification

A) The SynBot selection menu serves as the primary point of user input to adjust options for synapse analysis.

B) The main steps in the SynBot colocalization analysis:

1) Images are loaded into the software and converted to RGB.
2) Images are denoised using the FIJI Subtract Background and Gaussian Blur Filter functions.
3) Each image channel is thresholded to separate synaptic puncta from the background.
4) A region of interest (ROI) for colocalization quantification can be selected (dashed-line).

5-6) Red and green puncta are detected by FIJI's Analyze Particles function and counted.

7) Colocalization between red and green puncta are calculated. See Figure 3.

8) The colocalized puncta are overlayed on the original image, and the data are saved as a .csv file.

The scale bar in the larger image represents 20 μm, and the scale bar in the smaller image represents 5 μm.

Figure 3: Detection and calculation of puncta colocalization

A) SynBot detects colocalizations between synaptic puncta by first calculating the distance between the centers of the puncta and then determining if that distance is less than the sum of the radii of the puncta. If this distance is less than the sum of the radii, the colocalization is recorded and the area of colocalization is calculated.

B) SynBot runs the following calculations for the area of colocalization area.

1) Calculate the distance between the center of the first puncta and the line of intersection.

2) Calculate the distances from the midpoint of the distance between the two puncta centers (d) to the intersection of the edges of the two puncta.

3) Calculates the area of the sector of the first puncta between the two intersection points.

4) Calculates the area of the sector for the second puncta.

5) Calculates the area of the rectangle formed by the two centers and intersection points; the sum of the two triangular portions of the sectors that are not part of the overlap.

6) The general form for the area of colocalization is the sum of the two sectors minus the two triangular portions outside of the overlap.

C) Pictorial representation of the pixel-overlap analysis mode where FIJI's image calculator is used to identify pixels that are part of both the red and green channel for a

2-channel colocalization or part of the red, green, and blue channels for a 3-channel colocalization. Scale bar represents 1 μm.

Figure 4: SynBot quantifies astrocyte-induced synapse formation *in vitro.*

A) Scheme of single cell suspension generation from P1 rat pup cortices.

B) Scheme of neuronal isolation by immunopanning first through a series of negative panning steps and then through positive panning with Anti-L1CAM antibody.

C) Scheme of astrocyte purification and astrocyte-conditioned media (ACM) preparation.

D) Timeline of neuronal feeding schedule and ACM treatment.

E) Representative images (in RGB) of excitatory synaptic puncta stained with presynaptic marker Bassoon and postsynaptic marker Homer1. Scale: 15 μm for full image and 3 μm for zoom in.

F) Example of quantification of excitatory synaptic colocalization between control and ACM using the Puncta Analyzer, SynBot manual thresholding, or SynBot ilastik thresholding. Student's T-test, 20 neurons per treatment. Error bars represent 1 standard error of the mean.

G) Representative images (in RGB) of inhibitory synaptic puncta stained with presynaptic marker Bassoon and postsynaptic marker Gephyrin. Scale: 15 μm for full image and 3 μm for zoom-in.

H) Example of quantification of inhibitory synaptic colocalization between control and ACM using the Puncta Analyzer, SynBot manual thresholding, or SynBot ilastik

thresholding. Student's T-test, 20 neurons per treatment. Error bars represent 1 standard error of the mean.

Figure 5: SynBot quantifies reduced α2δ-1 KO synapse numbers *in vivo*.

A) Workflow for harvesting mouse brain tissue and preparing it for synapse imaging.
B) Representative images of synapses from layer 2/3 of primary visual cortex in α2δ-1 wild type vs. α2δ-1 knockout mice at postnatal day 21. Magenta = VGluT1; Green = PSD95
C) Quantification of VGluT1-PSD95 colocalization using the Puncta Analyzer, SynBot manual thresholding, or SynBot ilastik thresholding. Colocalized puncta counts were normalized to the WT average for each experimental pair. A linear mixed-effects model was used to account for multiple images per animal. Mouse averages are shown as large black dots (N = 3 mice per condition) with individual images shown as small gray dots. Error bars represent 1 standard error of the mean.

Methods

RESOURCE AVAILABILITY

Lead contact

Further information and requests for resources and reagents should be directed to and will be fulfilled by the lead contact, Cagla Eroglu (cagla.eroglu@duke.edu).

Materials availability

This study did not generate new unique reagents.

Data and code availability

- Microscopy data reported in this paper will be shared by the lead contact upon request.
- All original code has been deposited at our lab Github site (https://github.com/Eroglu-Lab/Syn_Bot) and is publicly available at Zenodo as of the date of publication. The DOI is listed in the Key Resources table.
- Any additional information required to reanalyze the data reported in this paper is available from the lead contact upon request.

Resources

REAGENT or RESOURCE	SOURCE	IDENTIFIER
Antibodies		
AffiniPure Goat anti-Rat IgG + IgM (H+L)	Jackson Immunoresearch	Cat# 112005044
AffiniPure Goat anti-Mouse IgG + IgM (H+L)	Jackson Immunoresearch	Cat# 115005044
Mouse anti-neural cell adhesion molecule L1 Hybridoma	Developmental Studies Hybridoma Bank	Cat# ASCS4
Anti-Bassoon antibody	Enzo/Assay Designs	Cat# SAP7F07/VAM-PS003F
Anti-Gephyrin antibody	Synaptic Systems	Cat# 147002
Anti-Homer1 antibody	Synaptic Systems	Cat# 160002
Anti-VGAT antibody	Synaptic Systems	Cat# 131004
Anti-Vglut1 antibody	Millipore	Cat# AB5905
Alexa Fluor 488 goat anti-Mouse IgG (H+L)	Invitrogen	Cat # A11001
Alexa Fluor 568 goat anti-Rabbit IgG (H+L)	Invitrogen	Cat# A11011
Alexa Fluor 647 goat anti-Guinea pig IgG (H+L)	Invitrogen	Cat# A21450
Guinea pig anti- VGAT	Synaptic Systems	Cat# 131004
Guinea pig anti- VGlut1	Sigma	Cat# AB5904
Guinea pig anti-VGlut2	Synaptic Systems	Cat# 135404
Rabbit anti-Gephyrin	Synaptic Systems	Cat# 147002

Rabbit anti-PSD95	Life Technologies	Cat# 51-6900
Chemicals, peptides, and recombinant proteins		
2,2,2-tribromoethanol	Sigma	Cat# T48402-25G
2-methyl-2-butanol	Sigma	Cat# 152463-250mL
B27	GIBCO	Cat# 17504044
B27 Plus	GIBCO	Cat# A3582801
BDNF	PeproTech	Cat# 450-02
Boric Acid	Sigma	Cat# B0394
BSA	Sigma	Cat# A4161
BSL1 (Baneiraea Simplicifolia Lectin 1)	Vector Laboratories	Cat# L-1100
CNTF	PeproTech	Cat# 450-13
Cytosine arabinoside (AraC)	Sigma	Cat# C1768
DAPI	Invitrogen	Cat#D1306
DMEM	GIBCO	Cat# 11960
DNaseI	Worthington	Cat# LS002007
DPBS with calcium, magnesium, glucose, and pyruvate	GIBCO	Cat# 14287
DPBS without calcium or magnesium	GIBCO	Cat# 14190144
Fetal Bovine Serum	Thermo Fisher	Cat# 10-437-028
Forskolin	Sigma	Cat# F6886
Glycerol	Acros Organics	Cat# 15892-0010
Hydrocortisone	Sigma	Cat# H-0888
Insulin	Sigma	Cat# 11882
L-Glutamine	GIBCO	Cat# 25030-081
Low protein binding tubes	Eppendorf	Cat# 022431081
Mouse Laminin	Cultrex	Cat# 3400-010-01
N-acetyl cysteine	Sigma	Cat# A8199
n-Propyl gallate	Sigma	Cat# P3130-100G
Neurobasal	GIBCO	Cat# 21103049
Neurobasal minus phenol red	GIBCO	Cat# 12348017
Neurobasal Plus	GIBCO	Cat# A3582901
Normal Goat Serum (NGS)	Thermo Fisher	Cat# 01-6201
Optimal Cutting Temperature solution (OCT)	Tissue Tek	Cat# 4583
Papain	Worthington	Cat# LK003178
Pen/Strep	GIBCO	Cat# 15140
PFA 16%	Electron Microscopy Sciences	Cat# 15710
Poly-D-Lysine	Sigma	Cat# P6407
Sodium Pyruvate	GIBCO	Cat# 11360-070
Tris Base	VWR	Cat# 101174-856
Triton X-100	Roche	Cat# 11332481001
Trypsin Inhibitor	Worthington	Cat# LS003083
Critical commercial assays		
Pierce BCA protein assay kit	Thermo Fisher	Cat# 23225
Experimental models: Cell lines		
Rat primary cortical neurons	This paper	N/A
Rat primary cortical astrocytes	This paper	N/A
Experimental models: Organisms/strains		

Rat: Sprague-Dawley	Charles River	001
Software and algorithms		
SynBot	This paper	Eroglu-Lab/Syn_Bot: Syn_Bot synapse calculation macro for FIJI (github.com)
FIJI	NIH	https://fiji.sc/
ilastik	Anna Kreshuk's lab (EMBL)	https://www.ilastik.org/
Puncta Analyzer	Ippolito and Eroglu, 2010	N/A
R: A Language and Environment for Statistical Computing	R Core Team	https://cran.r-project.org/
R package nlme	R Core Team	https://www.rdocumentation.org/packages/nlme/versions/3.1-162
Other		
20µm nylon mesh	Elko filtering	Cat# 03-20/14
Vivaspin MWCO 5000; 20 mL tubes	Sartorius	Cat # VS2012

EXPERIMENTAL MODEL AND SUBJECT DETAILS

Animals

Mice and rats were used for experiments as specified in the text and figure legends. All mice and rats were used in accordance with the Institutional Animal Care and Use Committee (IACUC) and the Duke Division of Laboratory Animal Resources (DLAR) oversight (IACUC Protocol Numbers A147-17-06 and A117-20-05). All mice and rats were housed under typical day/night conditions of 12-hour cycles. For all experiments, age, and sex-matched mice were randomly assigned to experimental groups based on genotypes. The primary rat neurons and astrocytes were isolated from wildtype Crl: CD(SD) Sprague-Dawley rats from Charles River Laboratories (RRID: RGD_734476).

METHOD DETAILS

In Vitro Synapse Assay with Astrocyte Conditioned Media

Cortical tissue digestion

Primary rat astrocytes and neurons were isolated from postnatal day 1 (P1) rat pups. Pups were rapidly decapitated, and brains dissected out and placed into a petri dish of PBS. Brains were then micro-dissected to isolate the cerebral cortex, and the cortices were chopped into pieces approximately 1 cubic millimeter in volume. A transfer pipet was then cut where it began to taper to create a larger opening. This cut pipet was then used to suck up the cortex chunks, and tissue was transferred to a tube of 7.5 units/mL papain digestion solution (Worthington, Cat# LK003178) by gently tapping on the pipette without depressing it. Cortices were then digested for 45 minutes at 33°C with a brief swirling at the 15- and 30-minute points. The digestion solution is then aspirated off and the tissue is resuspended in a 2 mg/ml trypsin inhibitor ovomucoid solution (Lo Ovo) (Worthington, Cat# LS003083). Cells were then spun in a centrifuge at 300g for 11 minutes at room temperature. The supernatant was then removed, and the cells were resuspended in a 4 mg/ml Ovomucoid solution (Hi Ovo). Cells were then spun again at 300g for 11 minutes and the supernatant removed. The resulting cells were then either used for isolating neurons or astrocytes according to the following sections.

Neuronal Isolation by Immunopanning

The pelleted cells from the cortical tissue digestion were resuspended in Panning Buffer (0.02% BSA with 0.5 ug/ml insulin in DPBS with calcium, magnesium, glucose, and pyruvate (Thermo Fisher, Cat# 14287080)). The cells were then filtered through a 20µm nylon mesh (Elko Filtering, Cat# 03-20/14) to remove clumps. These filtered cells were then added to a petri dish which had been treated with Griffonia Simplicifolia Lectin I (Vector Laboratories, Cat# L-1100) for 1 hour at room temperature prior to adding the

cells. The cells were incubated on this lectin plate for 10 minutes at room temperature. The plate was then forcefully shaken to resuspend any loosely adhered cells. The solution in the lectin plate was then transferred to a second lectin plate for a 15-minute incubation at room temperature. The second lectin plate was then forcefully shaken, and the solution transferred to a plate treated with an L1CAM antibody (α-L1) (Developmental Studies Hybridoma Bank, Cat# ASCS4) which binds to neurons. The cells were incubated on the α-L1 plate for 45 minutes at room temperature. The media was then gently removed from the α-L1 plate and the plate was washed 5 times with panning buffer. Cells bound to the α-L1 plate were then resuspended in the panning buffer and collected in a conical tube. The cells were then spun for 11 minutes at 300g. The supernatant was removed, and the cells were resuspended in neuronal growth media (NGM: Neurobasal (Gibco, Cat# 21103049), B27 supplement (Gibco, Cat# 17504044), 2 mM L-Glutamine (Gibco, Cat# 25030-081), 100 U/mL Pen/Strep (Gibco, Cat# 15140), 1 mM sodium pyruvate (Gibco, Cat# 11360-070), 4.2 μg/mL Forskolin (Sigma, Cat# F6886), 50 ng/mL BDNF (PeproTech, Cat# 450-02), and 10 ng/mL CNTF (PeproTech, Cat# 450-13)). The cells were then counted, and 60,000 cells each were plated onto poly-D-lysine-treated (Sigma, Cat# P6407) and mouse laminin (Cultrex, Cat# 3400-010-01) treated glass coverslips in a 24-well plate with neuronal growth media. Cells were then kept in a tissue culture incubator at 37°C with 10% CO_2.

Astrocyte Isolation and ACM Production

The pelleted cells from the cortical tissue digestion were resuspended in astrocyte growth media (AGM: DMEM (GIBCO, Cat# 11960), 10% FBS (Thermo Fisher, Cat# 10-437-028), 10 mM, hydrocortisone (Sigma, Cat# H-0888) , 100 U/mL Pen/Strep, 2 mM L-

Glutamine, 5 mg/mL Insulin (Sigma, Cat# 11882), 1 mM Sodium Pyruvate, 5 mg/mL N-Acetyl-L-cysteine (Sigma, Cat# A8199)). The cells were then filtered through a 20µm nylon mesh to remove cell clumps. The filtered cells were then spun for 9 minutes at 300g. The supernatant was then removed, and the cells were resuspended in AGM and counted. 15 million cells were then plated in a T-75 flask with a non-aerating top. Cells were then kept in a tissue culture incubator at 37°C with 10% CO_2 with the cap slightly unscrewed to allow airflow.

On DIV3, astrocyte flasks were washed 3 times with DPBS without calcium or magnesium (Gibco, Cat# 14190144). After the third wash, 20 mL of DPBS without calcium or magnesium was added and the flask was vigorously shaken to remove loosely adherent cells. This shake-off process significantly enriches for astrocytes. Media was then replaced with AGM and flasks were returned to their incubator. On DIV 5, astrocytes were treated with 2.43 mg/ml Cytosine arabinoside (AraC) (Sigma, Cat# C1768) through a full media change. On DIV 7 astrocytes were passaged using 0.05% Trypsin-EDTA. 3 million cells each were then plated into 10 cm culture dishes. On DIV 9, astrocytes were switched to a minimal media (Neurobasal medium minus phenol red (Gibco, Cat# 12348017), 100 U/mL pen/strep, 2mM L-glutamine, and 1mM sodium pyruvate) for astrocyte conditioning. Astrocytes were then cultured for 5 days without any media change, and on DIV 14, the ACM was collected. The ACM was then centrifuged for 5 minutes at 1,100g to pellet cellular debris. The supernatant was concentrated by centrifugation for 1 hour at 3220 g at 4°C in a 5kDa Cutoff Vivaspin tube (Sartorius, Cat # VS2012). ACM was aliquoted into low protein binding tubes (~100ul per aliquot), flash-frozen in liquid nitrogen, and stored at -80°C until use. An aliquot of each batch of ACM

was thawed and used to measure the protein content using the Pierce BCA protein assay kit (Thermo Fisher, Cat# 23225).

Neuron Feeding and ACM Treatment

On DIV2, neurons were treated with 2.43 mg/ml AraC through a half-media change. A full media change was then performed 24 hours later (DIV3) to remove the AraC. Neurons were then given another half-media change on DIV6. Neurons were then fed with ACM on DIV8 and DIV 11 by adding either 50 mg/ml ACM for excitatory synapses or 100 mg/ml ACM for inhibitory synapses in a half media change.

Neuron Staining and Imaging

On DIV 13, neurons were fixed with 4% paraformaldehyde (Electron Microscopy Sciences, Cat# 15710) in PBS. Cells were then washed 3 times with PBS and then blocked for 30 minutes at room temperature with antibody blocking buffer (150 mM NaCl, 50 mM Tris-Base, 1% BSA, 100 mM L-lysine 50% normal goat serum (Thermo Fisher, Cat# 01-6201), 0.2% Triton (Roche, Cat# 11332481001). The blocking buffer was then removed, and cells were incubated with primary antibodies against the pre- and post-synaptic markers of interest overnight at 4°C in antibody incubation buffer (150 mM NaCl, 50 mM Tris-Base (VWR, Cat# 101174-856), 1% BSA, 100 mM L-lysine, 10% normal goat serum). The following day cells were washed 3 times with PBS and incubated in fluorescent secondary antibodies in antibody incubation buffer for 2 hours at room temperature protected from light. Cells were then washed with PBS 3 times and incubated with 1:10,000 DAPI (Invitrogen, Cat#D1306) for 5 minutes. Cells were then washed 3 times with PBS and mounted onto coverslips with homemade mounting media (20mM Tris pH 8.0, 90% Glycerol, 0.5% N-propyl gallate) and sealed with nail polish.

Single focal plane images were taken using an inverted Olympus FV3000 confocal laser scanning microscope with a 60X oil immersion objective. The images were taken in a 1024X1024 resolution with a 2X digital zoom. For the picture acquisition, the DAPI channel was used to select neuronal cell bodies distant from other neurons to avoid overlap of cell soma and to do a blind selection of the neurons. DAPI positive nuclei with abnormal morphology were excluded for the analysis. 20 cells for each condition were selected for the analysis. Images were also saved as .bmp extension with only Bassoon (green) and Gephyrin (red channel) for the synaptic analysis.

Mouse Brain Tissue Synapse Assay

Mouse perfusion and cryosectioning

P21 α2δ-1 WT and KO mice were euthanized by intraperitoneal injection of 0.6mL of 12.5 mg/mL 2,2,2-tribromoethanol (Avertin) (Sigma, Cat# T48402-25G) followed by exsanguination through transcardially perfusion of tris-buffered saline (TBS: 137mM NaCl, 2.68 mM KCl, 24.8 mM Tris-base (Thermo Fisher, Cat# J75825.A7)). Following TBS perfusion, animals were perfused with warm, 4% paraformaldehyde (PFA) in TBS solution. Brains were then removed and post-fixed in 4% PFA overnight at 4°C. After post-fixation, brains were washed 3 times with TBS and then incubated in 30% sucrose in TBS for 48-72 hours. Brains are fully cryopreserved once they sink to the bottom of their container in the 30% sucrose. Brains were then placed in cryomolds and frozen in 50% Optimal Cutting Temperature Compound (OCT) (Tissue Tek, Cat# 4583) in TBS on dry ice. Brains were then kept at -80°C until sectioning. Brains were cryosectioned to a thickness of 15-40 μm and stored in 50% glycerol (Acros Organics, Cat# 15892-0010) in TBS at -20°C.

Tissue Section Synapse Staining and Imaging

Three tissue sections per animal were washed 3 times for ten minutes with 0.2% TritonX-100 in TBS (TBST) on a shaker at room temperature. Sections were then blocked with 5% normal goat serum in TBST for 1 hour at room temperature on a shaker. Sections were then stained with primary antibodies for the pre and postsynaptic markers of interest overnight at 4°C on a shaker. Sections were then washed 3 times in TBST for 10 minutes and incubated with fluorescent secondary antibodies for 2 hours at room temperature on a shaker protected from light. After secondary incubation, sections were washed 3 times with TBST for 10 minutes. After washing, sections were mounted onto microscope slides and sealed with nail polish.

Stained tissue is ready to image after nail polish is dried and should be imaged within 48 hours of secondary staining for most accurate results. Images were acquired using a Leica SP5 confocal microscope with a 63X oil immersion objective. For 1024 X 1024 images, a 1.64X digital zoom was used to achieve an XY resolution of 0.126 um X 0.126 µm pixel size and a z-stack of 15 optical planes was acquired using a 0.34 µm z-step to image ~ 5 µm of the sample. In general, images were acquired such that confocal settings were optimized on control conditions with the goal of minimizing oversaturated pixels but maintaining real synaptic puncta.

Image Analysis

Synapse Quantification with Puncta Analyzer

In vitro synapse assay images were analyzed using Puncta Analyer[38] by first converting the images to the RGB format and then running the Puncta Analyzer plugin on each image. A circular ROI was applied to each image with a radius of 301 pixels around the cell body of the imaged neuron. A threshold for each image was chosen to minimize the background while preserving the signal.

In vivo, synapse assay images were Z-projected such that every 3 optical planes were projected to produce 5 max-projections corresponding to 1 μm, per 15-image stack covering the 5 μm. Images were then analyzed with the Puncta Analyzer plugin using default settings. A threshold for each image was chosen by users to minimize the background while preserving the signal.

Synapse Quantification with SynBot

Images were analyzed with the SynBot macro using the default settings for the manual thresholding method. A threshold for each image was chosen to minimize the background while preserving the signal. Threshold performance was checked visually using the "_colocs" image SynBot creates that displays which puncta were counted as synapses in each image.

For the ilastik thresholding method, images were first preprocessed into individual color channels using the extract_channels macro (available at https://github.com/Eroglu-Lab/Syn_Bot). These single-channel images were then used to train ilastik projects for each image channel. Each ilastik project was trained using the pixel classification mode in ilastik. A random subset of images from the target color channel was chosen for the training set. For both *in vitro* and *in vivo* synapse analysis, we used all the image features available. We then annotated approximately 20 synapses as label 1 and marked several

regions of the background as label 2 on the first image. We then used the live update feature to view the classifications of each pixel and added additional annotations to the first image and subsequent images as necessary. We then saved the ilastik project files and used these for the SynBot ilastik thresholding method (all ilastik project files used for this paper are available at https://github.com/Eroglu-Lab/Syn_Bot).

QUANTIFICATION AND STATISTICAL ANALYSES

SynBot was used to quantify synapse numbers in the experiments shown. Subsequent statistical analysis was performed with the R statistical software (R Core Team). Student's t-tests were used to test for significance between conditions for the *in vitro* experiments, and linear mixed-effects models were used (R package nlme, R Core Team) to test the significance of *in vivo* experiments and account for the nested structure of the data (multiple z-stacks per image and multiple images per animal). Statistical details of each experiment can be found in the figure legends. For the cell culture experiments, each n represents a neuron that was imaged. For mouse tissue sections experiments, each n represents the average synapse density of a mouse that was included in the experiment. For each mouse, at least 15 max-projection images corresponding to 3 independent z-stacks were used. The full R code for performing the statistical analyses and producing the plots in this paper is available at https://github.com/Eroglu-Lab/Syn_Bot.

References

1. Farhy-Tselnicker, I. & Allen, N. J. Astrocytes, neurons, synapses: a tripartite view on cortical circuit development. *Neural Dev* **13**, (2018).

2. Cadwell, C. R., Bhaduri, A., Mostajo-Radji, M. A., Keefe, M. G. & Nowakowski, T. J. Development and Arealization of the Cerebral Cortex. *Neuron* **103**, 980–1004 (2019).

3. Pan, Y. & Monje, M. Activity Shapes Neural Circuit Form and Function: A Historical Perspective. *Journal of Neuroscience* **40**, 944–954 (2020).

4. Luo, L. Architectures of Neuronal Circuits. *Science* **373**, eabg7285 (2021).

5. Batool, S. *et al.* Synapse formation: From cellular and molecular mechanisms to neurodevelopmental and neurodegenerative disorders. *J Neurophysiol* **121**, 1381–1397 (2019).

6. Rizalar, F. S., Roosen, D. A. & Haucke, V. A Presynaptic Perspective on Transport and Assembly Mechanisms for Synapse Formation. *Neuron* **109**, 27–41 (2021).

7. Groc, L. & Choquet, D. Linking glutamate receptor movements and synapse function. *Science (1979)* **368**, (2020).

8. Newschaffer, C. J. *et al.* An Overview of the Main Genetic, Epigenetic and Environmental Factors Involved in Autism Spectrum Disorder Focusing on Synaptic Activity. *International Journal of Molecular Sciences 2020, Vol. 21, Page 8290* **21**, 8290 (2020).

9. Pocklington, A. J., O'Donovan, M. & Owen, M. J. The synapse in schizophrenia. *European Journal of Neuroscience* **39**, 1059–1067 (2014).

10. Lane-Donovan, C. & Herz, J. ApoE, ApoE Receptors, and the Synapse in Alzheimer's Disease. *Trends in Endocrinology & Metabolism* **28**, 273–284 (2017).

11. Rizo, J. & Xu, J. The Synaptic Vesicle Release Machinery. *Annu Rev Biophys* **44**, 339–367 (2015).

12. Rusakov, D. A., Savtchenko, L. P., Zheng, K. & Henley, J. M. Shaping the synaptic signal: molecular mobility inside and outside the cleft. *Trends Neurosci* **34**, 359–369 (2011).

13. Luján, R., Shigemoto, R. & López-Bendito, G. Glutamate and GABA receptor signalling in the developing brain. *Neuroscience* **130**, 567–580 (2005).

14. Vyklicky, V. *et al.* Structure, function, and pharmacology of NMDA receptor channels. *Physiol Res* **63**, (2014).

15. Diering, G. H. & Huganir, R. L. The AMPA Receptor Code of Synaptic Plasticity. *Neuron* **100**, 314–329 (2018).

16. Chen, H., Tang, A. H. & Blanpied, T. A. Subsynaptic spatial organization as a regulator of synaptic strength and plasticity. *Curr Opin Neurobiol* **51**, 147–153 (2018).

17. Iasevoli, F., Tomasetti, C. & De Bartolomeis, A. Scaffolding proteins of the post-synaptic density contribute to synaptic plasticity by regulating receptor localization and distribution: relevance for neuropsychiatric diseases. *Neurochem Res* **38**, 1–22 (2013).

18. Akin, O. & Zipursky, S. L. Activity regulates brain development in the fly. *Curr Opin Genet Dev* **65**, 8–13 (2020).

19. Andreae, L. C. & Burrone, J. The role of neuronal activity and transmitter release on synapse formation. *Curr Opin Neurobiol* **27**, 47–52 (2014).

20. Chen, L. F., Zhou, A. S. & West, A. E. Transcribing the connectome: roles for transcription factors and chromatin regulators in activity-dependent synapse development. *J Neurophysiol* **118**, 755–770 (2017).

21. Shen, K. & Scheiffele, P. Genetics and cell biology of building specific synaptic connectivity. *Annu Rev Neurosci* **33**, 473–507 (2010).

22. Sanes, J. R. & Zipursky, S. L. Synaptic Specificity, Recognition Molecules, and Assembly of Neural Circuits. *Cell* **181**, 536–556 (2020).

23. Jain, S. & Zipursky, S. L. Temporal control of neuronal wiring. *Semin Cell Dev Biol* (2022) doi:10.1016/J.SEMCDB.2022.05.012.

24. Farhy-Tselnicker, I. *et al.* Activity-dependent modulation of synapse-regulating genes in astrocytes. *Elife* **10**, (2021).

25. Wilton, D. K., Dissing-Olesen, L. & Stevens, B. Neuron-Glia Signaling in Synapse Elimination. *Annu Rev Neurosci* **42**, 107–127 (2019).

26. Chung, W. S., Allen, N. J. & Eroglu, C. Astrocytes Control Synapse Formation, Function, and Elimination. *Cold Spring Harb Perspect Biol* **7**, (2015).

27. Bonetto, G., Belin, D. & Káradóttir, R. T. Myelin: A gatekeeper of activity-dependent circuit plasticity? *Science* **374**, (2021).

28. Sancho, L., Contreras, M. & Allen, N. J. Glia as sculptors of synaptic plasticity. *Neurosci Res* **167**, 17–29 (2021).

29. Allen, N. J. & Eroglu, C. Cell Biology of Astrocyte-Synapse Interactions. *Neuron* **96**, 697–708 (2017).

30. Baldwin, K. T. & Eroglu, C. Molecular mechanisms of astrocyte-induced synaptogenesis. *Curr Opin Neurobiol* **45**, 113–120 (2017).

31. Tan, C. X., Burrus Lane, C. J. & Eroglu, C. Role of astrocytes in synapse formation and maturation. *Curr Top Dev Biol* **142**, 371–407 (2021).

32. Watanabe, S. *et al.* Clathrin regenerates synaptic vesicles from endosomes. *Nature 2014 515:7526* **515**, 228–233 (2014).

33. Begemann, I. & Galic, M. Correlative light electron microscopy: Connecting synaptic structure and function. *Frontiers in Synaptic Neuroscience* vol. 8 Preprint at https://doi.org/10.3389/fnsyn.2016.00028 (2016).

34. Staffler, B. *et al.* SynEM, automated synapse detection for connectomics. *Elife* **6**, (2017).

35. Dorkenwald, S. *et al.* Automated synaptic connectivity inference for volume electron microscopy. *Nature Methods 2017 14:4* **14**, 435–442 (2017).

36. Chandrasekaran, S. *et al.* Unbiased, High-Throughput Electron Microscopy Analysis of Experience-Dependent Synaptic Changes in the Neocortex. *Journal of Neuroscience* **35**, 16450–16462 (2015).

37. Segev, A., Garcia-Oscos, F. & Kourrich, S. Whole-cell Patch-clamp Recordings in Brain Slices. *J Vis Exp* **2016**, 54024 (2016).

38. Ippolito, D. M. & Eroglu, C. Quantifying Synapses: an Immunocytochemistry-based Assay to Quantify Synapse Number. *JoVE (Journal of Visualized Experiments)* e2270 (2010) doi:10.3791/2270.

39. Maidorn, M., Rizzoli, S. O. & Opazo, F. Tools and limitations to study the molecular composition of synapses by fluorescence microscopy. *Biochem J* **473**, 3385–3399 (2016).

40. Blanco-Suarez, E., Liu, T. F., Kopelevich, A. & Allen, N. J. Astrocyte-Secreted Chordin-like 1 Drives Synapse Maturation and Limits Plasticity by Increasing Synaptic GluA2 AMPA Receptors. *Neuron* **100**, 1116-1132.e13 (2018).

41. Stogsdill, J. A. *et al.* Astrocytic neuroligins control astrocyte morphogenesis and synaptogenesis. *Nature* **551**, 192–197 (2017).

42. Holt, L. M. *et al.* Astrocyte morphogenesis is dependent on BDNF signaling via astrocytic TrkB.T1. *Elife* **8**, (2019).

43. Nguyen, A. Q. *et al.* Astrocytic Ephrin-B1 Controls Excitatory-Inhibitory Balance in Developing Hippocampus. *J Neurosci* **40**, 6854–6871 (2020).

44. Glebov, O. O., Cox, S., Humphreys, L. & Burrone, J. Neuronal activity controls transsynaptic geometry. *Scientific Reports 2016 6:1* **6**, 1–11 (2016).

45. Baldwin, K. T. *et al.* HepaCAM controls astrocyte self-organization and coupling. *Neuron* (2021) doi:10.1016/j.neuron.2021.05.025.

46. Nguyen, A. Q. *et al.* Astrocytic Ephrin-B1 Controls Excitatory-Inhibitory Balance in Developing Hippocampus. *J Neurosci* **40**, 6854–6871 (2020).

47. Verstraelen, P., Garcia-Diaz Barriga, G., Larsen, P. H., Timmermans, J.-P. & De Vos, W. H. Systematic Quantification of Synapses in Primary Neuronal Culture. *iScience* **23**, 101542 (2020).

48. McNamara, G., Difilippantonio, M., Ried, T. & Bieber, F. R. Microscopy and Image Analysis. *Curr Protoc Hum Genet* **94**, 4.4.1-4.4.89 (2017).

49. Dani, A., Huang, B., Bergan, J., Dulac, C. & Zhuang, X. Superresolution Imaging of Chemical Synapses in the Brain. *Neuron* **68**, 843–856 (2010).

50. Risher, W. C. *et al.* Astrocytes refine cortical connectivity at dendritic spines. *Elife* **3**, (2014).

51. Risher, W. C. *et al.* Thrombospondin receptor α2δ-1 promotes synaptogenesis and spinogenesis via postsynaptic Rac1. *Journal of Cell Biology* **217**, 3747–3765 (2018).

52. Berg, S. *et al.* ilastik: interactive machine learning for (bio)image analysis. *Nat Methods* **16**, 1226–1232 (2019).

53. Eisele, R. Calculate the intersection area of two circles. https://www.xarg.org/2016/07/calculate-the-intersection-area-of-two-circles/ (2016).

54. Irala, D. *et al.* Astrocyte-Secreted Neurocan Controls Inhibitory Synapse Formation and Function 2. *bioRxiv* (2023) doi:10.1101/2023.04.03.535448.

55. Singh, S. K. *et al.* Astrocytes Assemble Thalamocortical Synapses by Bridging NRX1α and NL1 via Hevin. *Cell* **164**, 183–196 (2016).

56. Allen, N. J. *et al.* Astrocyte glypicans 4 and 6 promote formation of excitatory synapses via GluA1 AMPA receptors. *Nature* **486**, 410–414 (2012).

57. Christopherson, K. S. *et al.* Thrombospondins are astrocyte-secreted proteins that promote CNS synaptogenesis. *Cell* **120**, 421–433 (2005).

58. Kucukdereli, H. *et al.* Control of excitatory CNS astrocyte-secreted protein. 43–45 (2016) doi:10.1073/pnas.1104977108.

59. Diniz, L. P. *et al.* Astrocyte-induced synaptogenesis is mediated by transforming growth factor β signaling through modulation of d-serine levels in cerebral cortex neurons. *Journal of Biological Chemistry* **287**, 41432–41445 (2012).

60. Risher, W. C. *et al.* Thrombospondin receptor α2δ-1 promotes synaptogenesis and spinogenesis via postsynaptic Rac1. *J Cell Biol* **217**, 3747 LP – 3765 (2018).

61. Eroglu, Ç. *et al.* Gabapentin Receptor α2δ-1 Is a Neuronal Thrombospondin Receptor Responsible for Excitatory CNS Synaptogenesis. *Cell* **139**, 380–392 (2009).

Figure 1

Savage et. al., 2023

A)

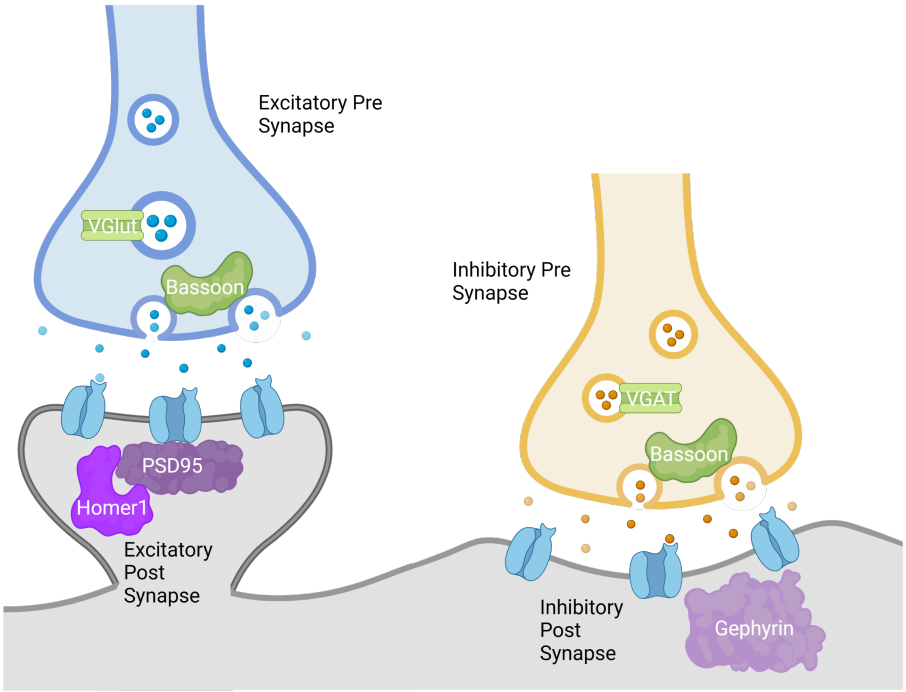

B)

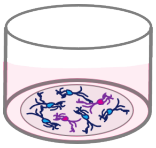

1) Permeabilization and blocking

	2) Primary antibody	**4) Secondary antibody**
Excitatory Synapses	Ms-α-Bassoon GP-α-VGluT1 Rb-α-Homer1	Gt-α-Ms Alexa 488 Gt-α-GP Alexa 647 Gt-α-Rb Alexa 564
Inhibitory Synapses	Ms-α-Bassoon GP-α-VGAT Rb-α-Gephyrin	Gt-α-Ms Alexa 488 Gt-α-GP Alexa 647 Gt-α-Rb Alexa 564

3) PBS Wash

5) PBS Wash and DAPI

6) Mounting

C) Excitatory Synapses

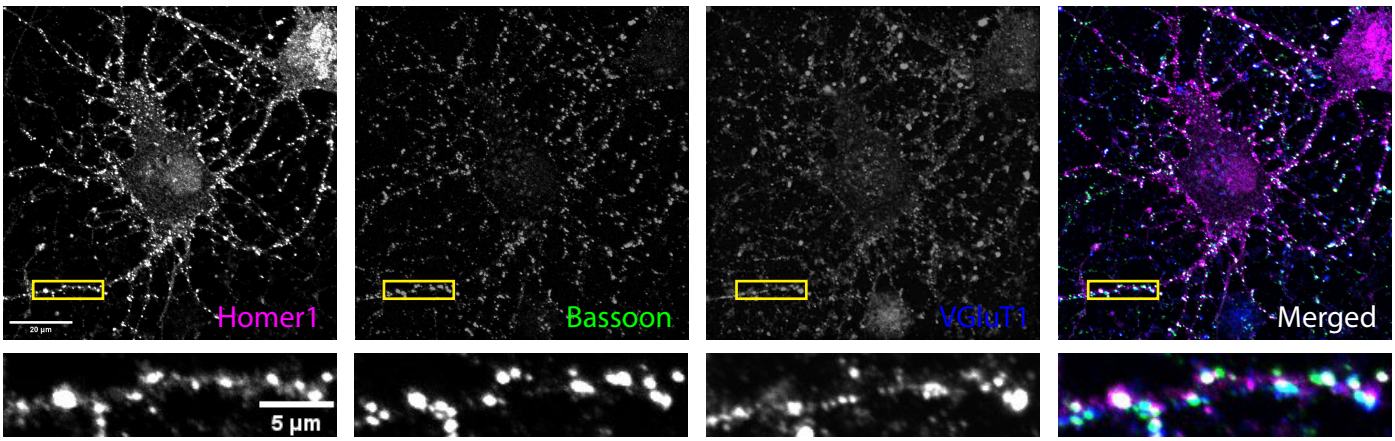

D) Inhibitory Synapses

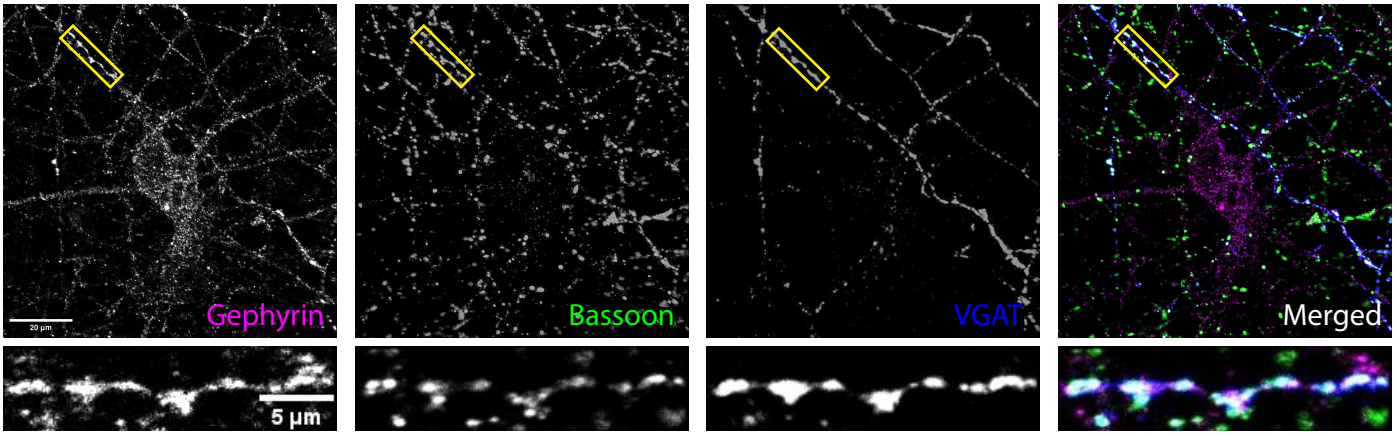

Figure 2

Savage et. al., 2023

A)

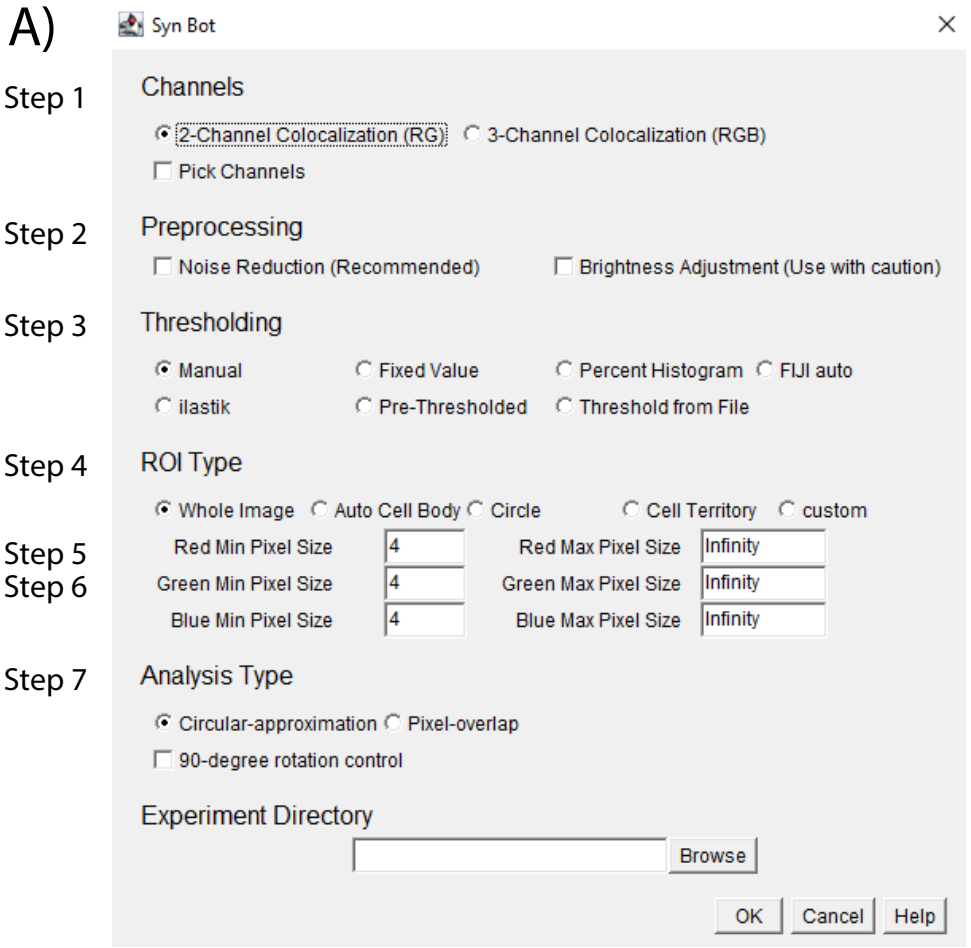

B)

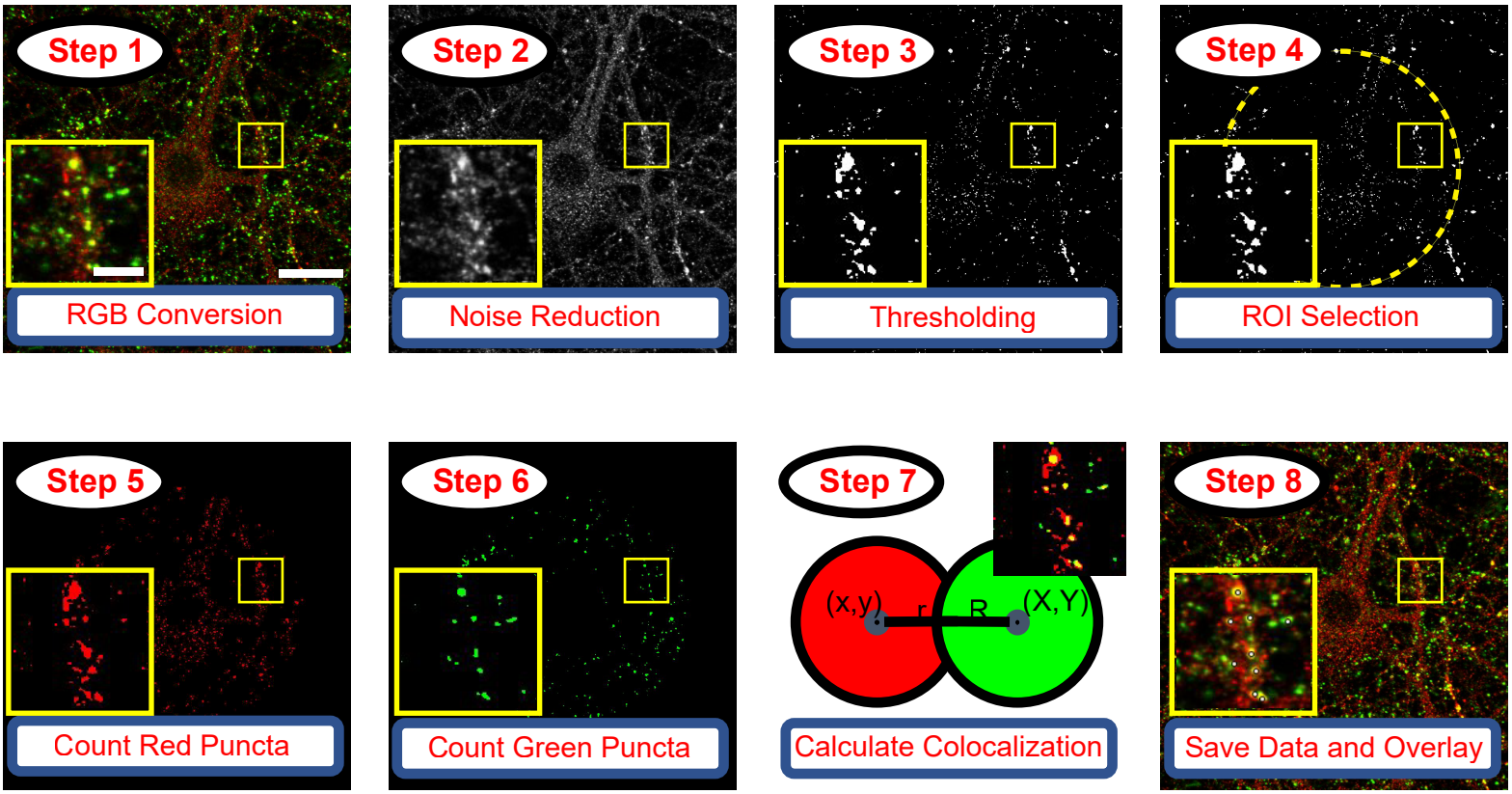

A)

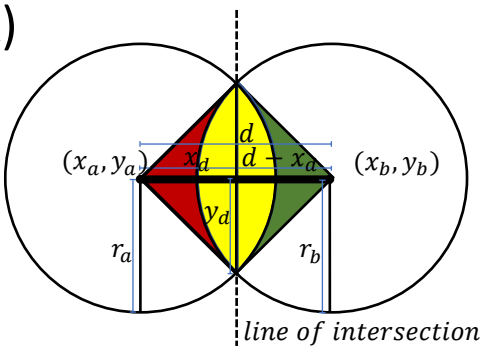

Distance between puncta centers $= d = \sqrt{(y_b - y_a)^2 + (x_b - x_a)^2}$

If $d < r_a + r_b$:

All colocalizations with any overlap are counted
If there is an overlap, the colocalization area is calculated

B)

Distance from x_a to the line of intersection $= x_d = \frac{(r_a^2 - r_b^2 + d^2)}{2d}$

Distance from the point of intersection to the midline $= y_d = \sqrt{r_a^2 - {x_d}^2}$

$= Sector_a = r_a^2 \cdot \sin^{-1}\left(\frac{y_d}{r_a}\right)$

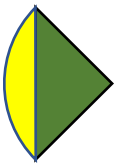

$= Sector_b = r_b^2 \cdot \sin^{-1}\left(\frac{y_d}{r_b}\right)$

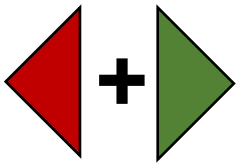

$= Triangles = y_d \cdot \left(x_d + \sqrt{{x_d}^2 + r_b^2 + r_a^2}\right)$

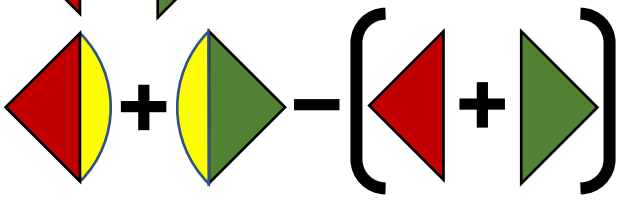

$= Area_{coloc} = Sector_a + Sector_b - Triangles$

C)

Red AND Green AND Blue = Triple Colocalization (White)

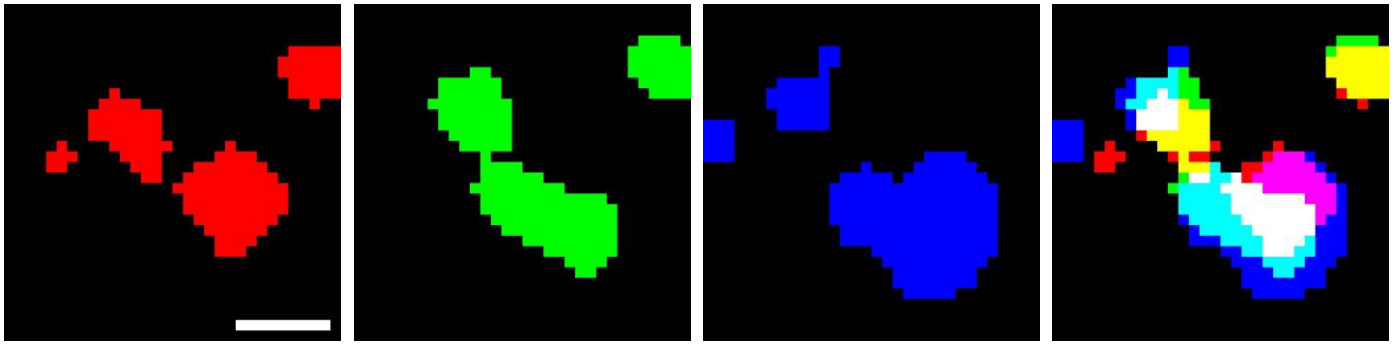

Figure 4

Savage et. al., 2023

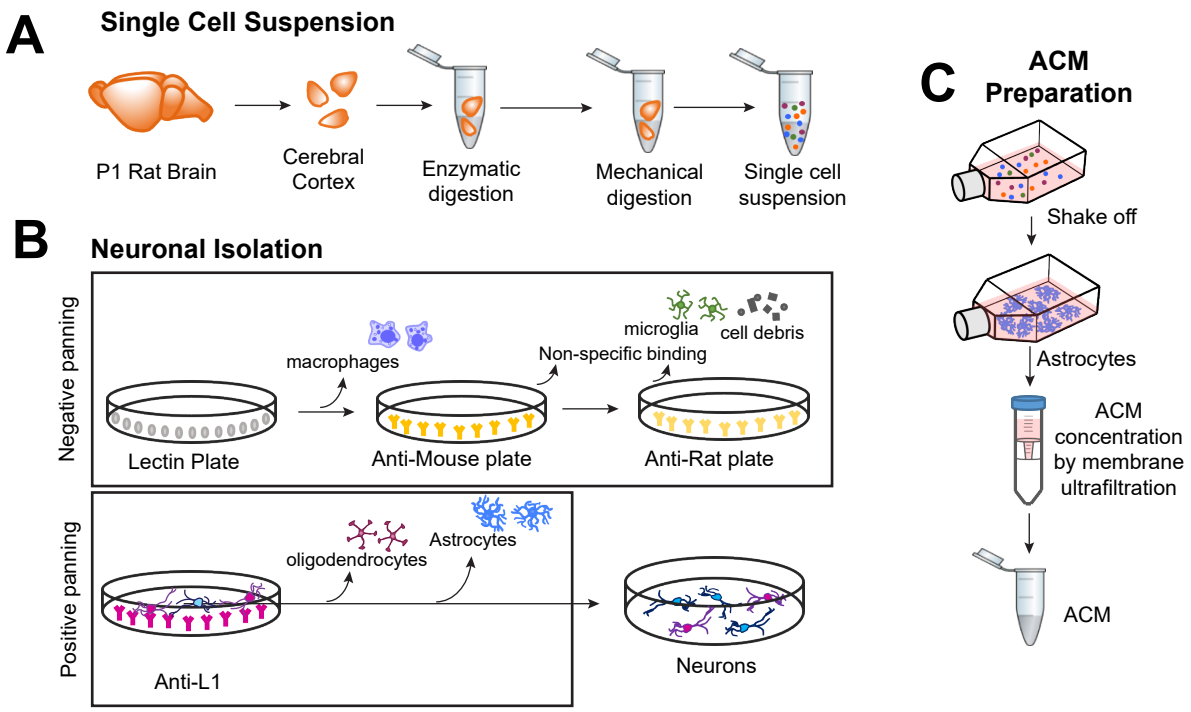

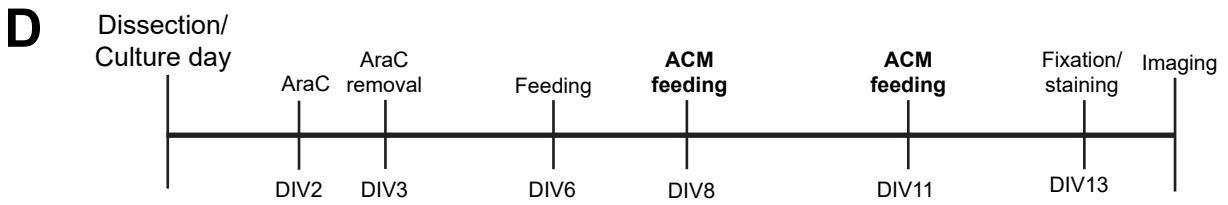

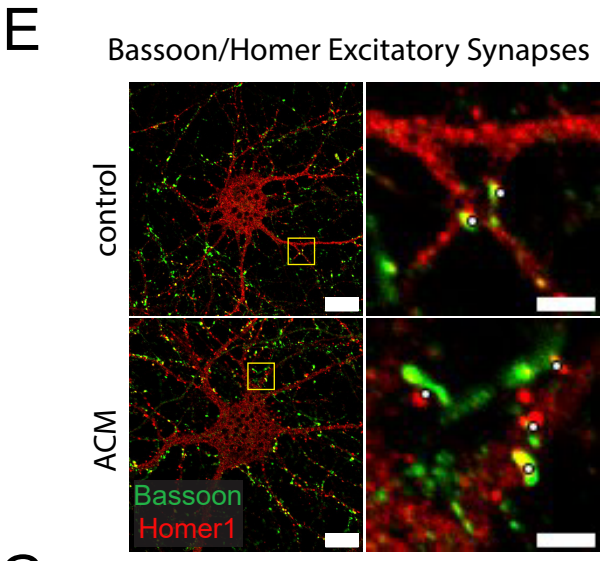

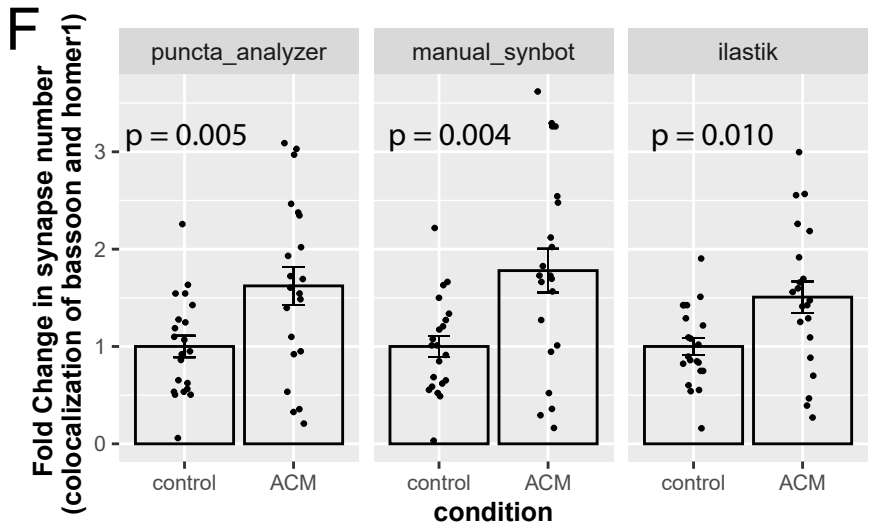

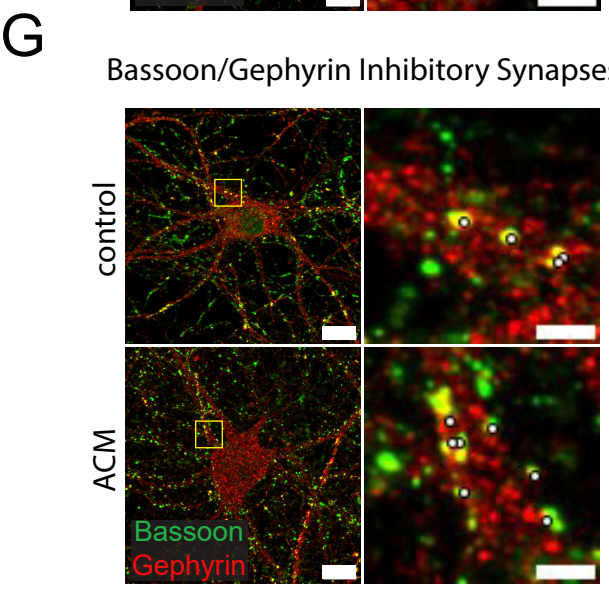

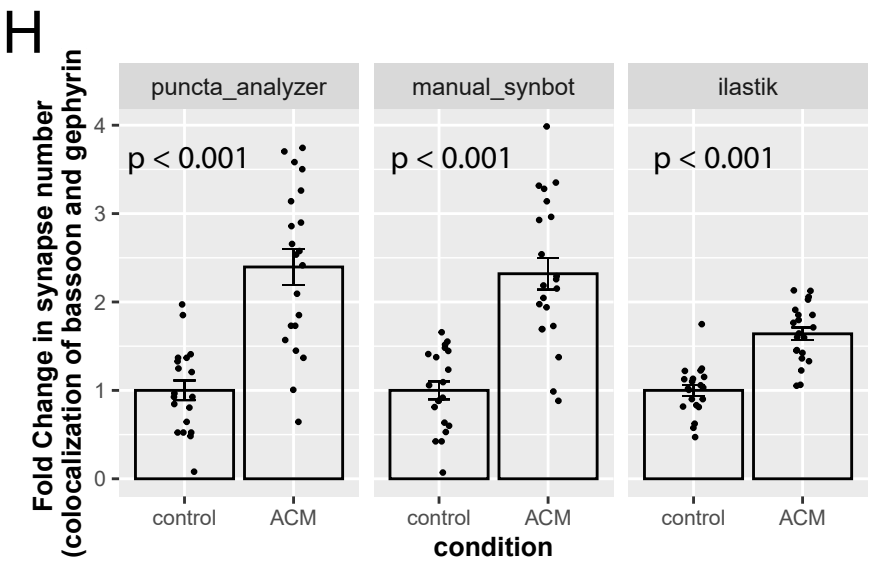

Figure 5

Savage et. al., 2023

A)

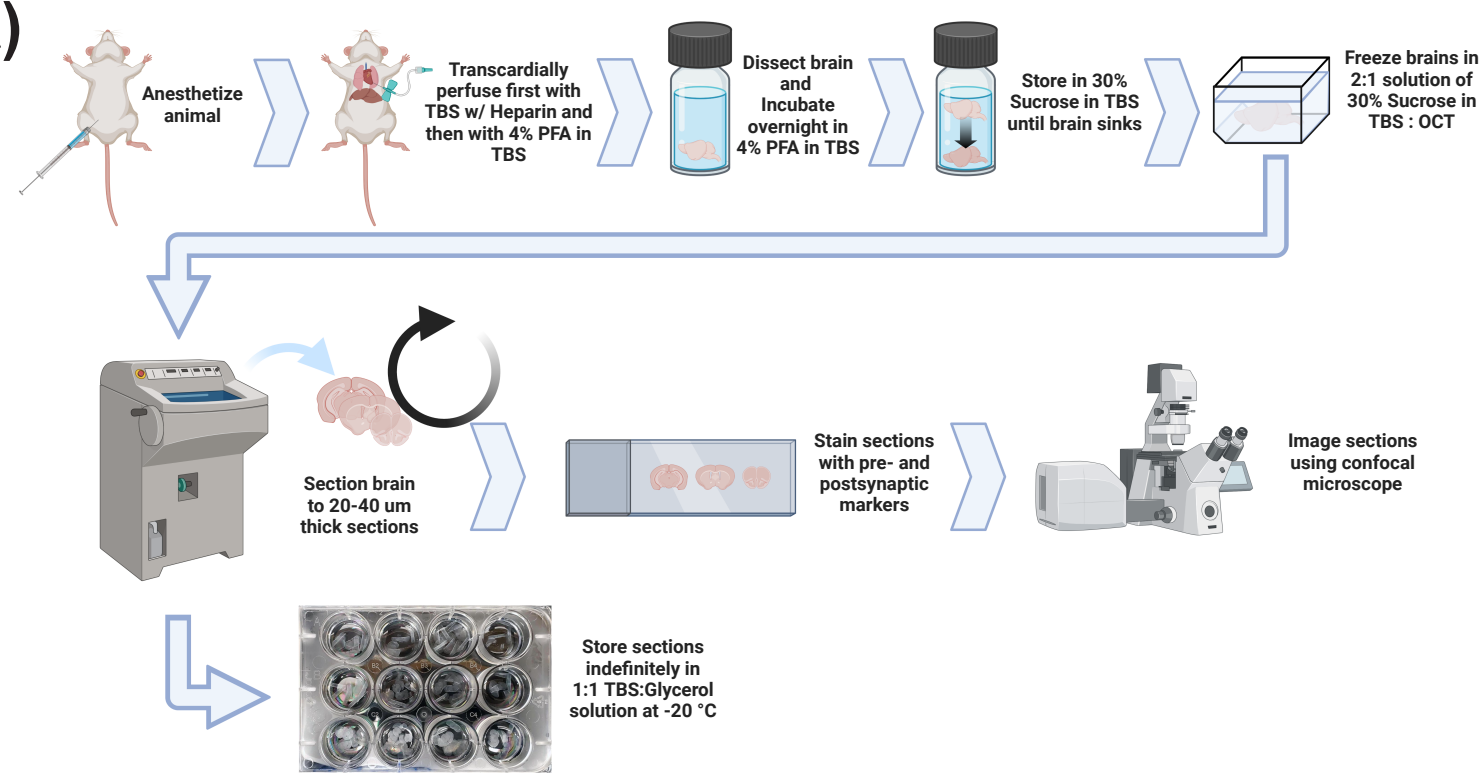

B)

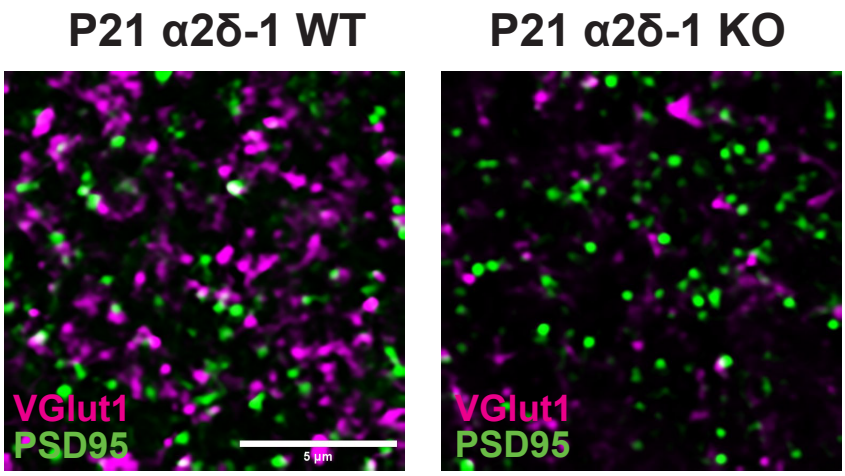

C)

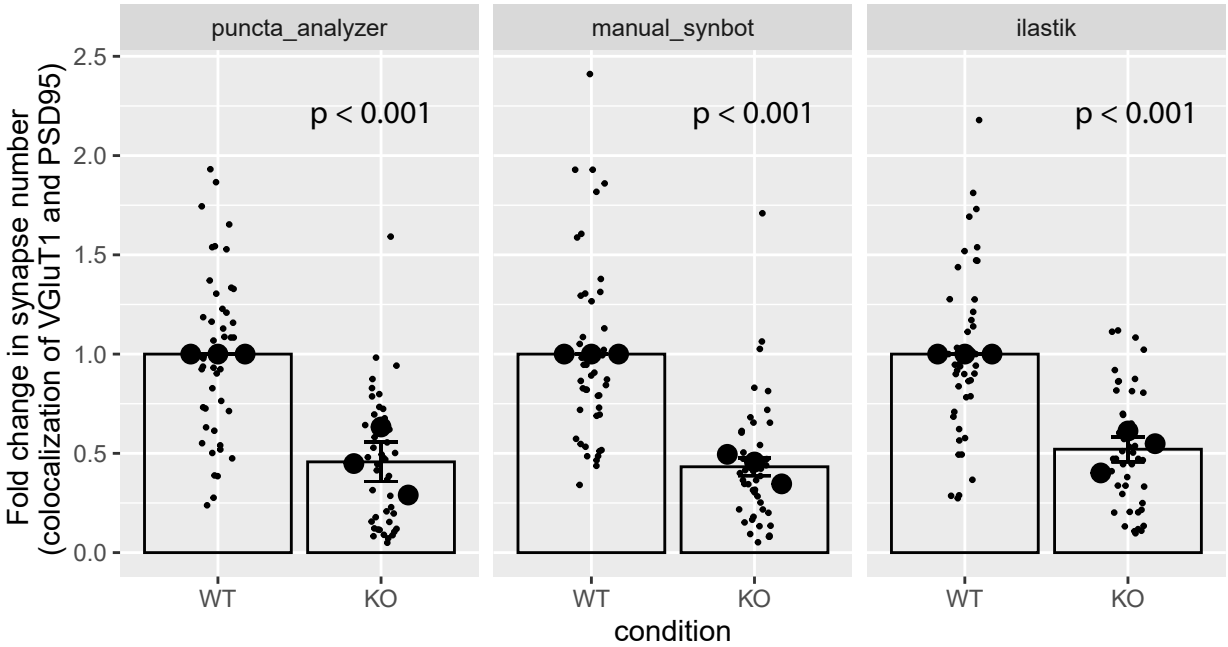

SUPPLEMENTAL INFORMATION

Table S1 SynBot Functions Defined Related to Figure 2

Step	Function Name	Description
1a	2-Channel Colocalization	The red and green image channels are analyzed for colocalizations.
1b	3-Channel Colocalization	The red, green, and blue image channels are analyzed for triple colocalizations.
1-	Pick Channels	This option allows the user to change the color of the channels in the input images. This is particularly useful since SynBot requires the input images to have the channels to be analyzed in red, green, and blue. SynBot will attempt RGB conversion without this option selected and may have unintended results such as splitting magenta signal across red and blue or analyzing the wrong channels.
2-	Noise Reduction (Recommended)	This option removes background by applying the FIJI Subtract Background function (rolling ball radius = 50) followed by a Gaussian Blur Filter (sigma = 0.57) to aid in object detection.
2-	Brightness Adjustment	This option adjusts the image brightness using the FIJI Enhance Contrast function to have a certain percentage of saturated pixels. This option is not recommended unless images are consistently dim across conditions. Consider adjusting imaging parameters.
3a	Manual	This thresholding method allows the user to manually threshold each channel of each image.
3b	Fixed Value	This thresholding method allows the user to set a single threshold value for each channel that is used for all of the images being analyzed.

3c	Percent Histogram	This thresholding method adjusts the image threshold such that the brightest pixels are kept. The percentage of pixels above threshold for each channel is provided by the user.
3d	FIJI auto	This thresholding method allows the user to apply any of the automated thresholding algorithms in the FIJI auto threshold function.
3e	ilastik	This thresholding method applies a user-trained random forest machine learning model for each channel to threshold the images. Training the model in ilastik is described in Berg et. al., 2019 *Nature Methods*. We recommend training the ilastik model on at least 5 images across conditions.
3f	Pre-Thresholded	This thresholding method allows users to input pre-thresholded images into SynBot.
3g	Threshold from File	This thresholding method allows users to enter a csv with threshold values to use for each channel of each image. Importantly, this feature can be used to replicate previous analyses and optimize other analysis parameters while keeping the thresholds the same.
4a	Whole Image	This ROI option analyzes the whole input image.
4b	Auto Cell Body	This ROI option can be used to identify a single cell body automatically and draw a circular ROI around it. This method does not work well if the image includes more than one cell. If this method fails SynBot will prompt the user to use the circle method.
4c	Circle	This ROI option allows the user to select a central point for each image and creates a circle ROI around that point with a set radius.
4d	Cell Territory	This ROI option can be used to automatically identify a cell's territory using a cell fill marker in

		the blue channel. A mask is created which serves as the ROI for red and green colocalization. This ROI method only works with the 2-Channel colocalization method selected in step 1.
4e	Custom	This ROI allows the user to set a custom ROI for each image.
5 & 6	Red/Green/Blue Min/Max Pixel Size	This field allows the user to set a minimum and maximum pixel area to be counted as a punctum for each channel.
7a	Circular-approximation	This analysis option calculates colocalizations by approximating red and green puncta to circles based on their radii and coordinates and using this to determine if they overlap.
7b	Pixel-overlap	This analysis option uses the FIJI Image Calculator function to identify pixels that contain red and green signal that is above threshold and counts these as colocalizations.
7-	90-degree rotation control	This option rotates the red image 90 degrees to the right and then performs the SynBot analysis as usual. This can be used as a control to test if the number of colocalization observed are greater than what would be seen by chance given the abundance of the red and green markers.
	Experiment Directory	This opens a file explorer dialog to select the image input folder.

Table S2 Circularity of Synaptic Markers Related to Figures 4 and 5

Corresponding Figure	Marker	Average Circularity (Range 0-1) +/- standard deviation

4 E & F	Homer1	0.882 +/- 0.0413
4 E & F	Bassoon	0.897 +/- 0.0162
4 G & H	Gephyrin	0.884 +/- 0.0223
4 G & H	Bassoon	0.911 +/- 0.0124
5 B & C	PSD95	0.922 +/- 0.0282
5 B & C	VGluT1	0.823 +/- 0.0314

Figure S1 Raw Puncta Counts by Analysis Method Related to Figures 4 and 5

Raw postsynaptic (red) puncta, presynaptic (green) puncta, and colocalized puncta counts for In Vitro Excitatory, In Vitro Inhibitory, and In Vivo a2d1 experiments related to Figures 4E, 4G, and 5C respectively. Lines indicate puncta counts for the same image across analysis methods. Control or WT images are on the left of each plot marked with solid lines and ACM or KO images are on the right side of each plot marked with dashed lines.

Figure S1
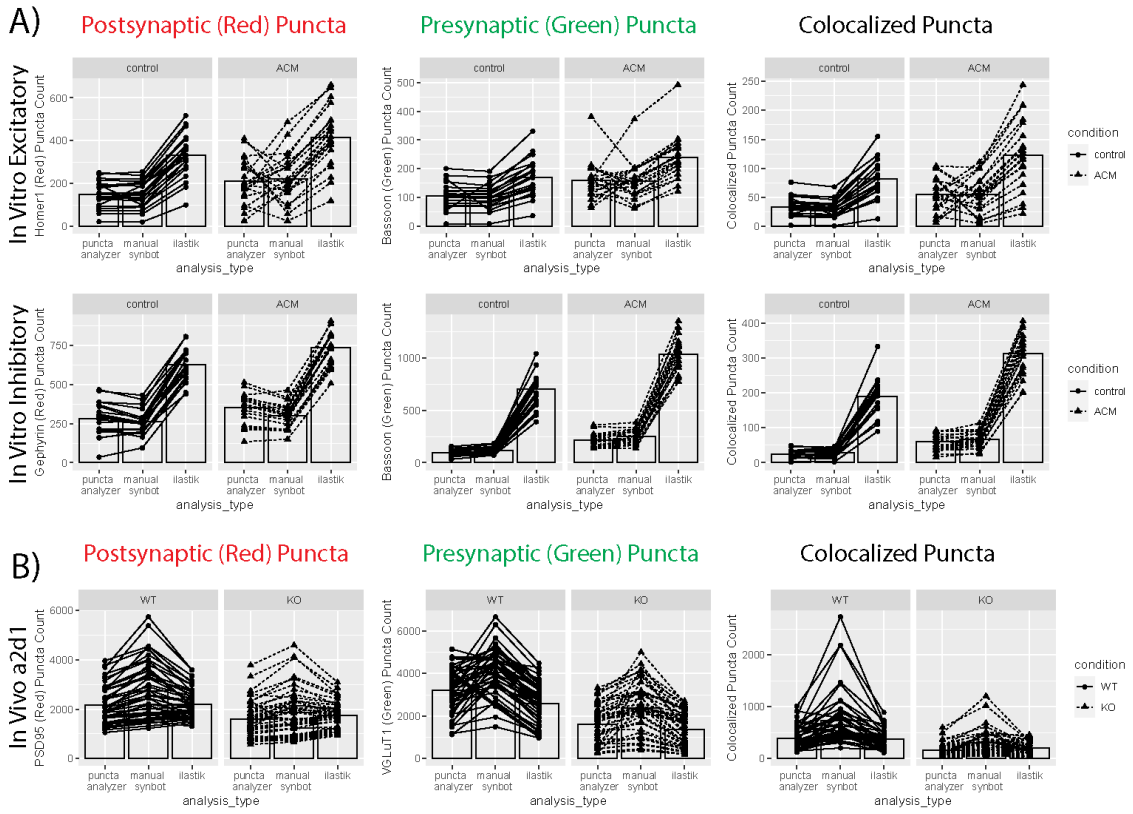
Savage et. al., 2023